



Multiple eco-regions contribute to the seasonal cycle of Antarctic aerosol size distributions

James Brean¹, David C. S. Beddows¹, Eija Asmi², Aki Virkkula^{2,3}, Lauriane L. J. Quéléver³, Mikko Sipilä³, Floortje Van Den Heuvel⁴, Thomas Lachlan-Cope⁴, Anna Jones⁴, Markus Frey⁴, Angelo Lupi⁵, Jiyeon Park⁶, Young Jun Yoon⁶, Rolf Weller⁷, Giselle L. Marincovich^{8,9}, Gabriela C. Mulena^{8,9}, Roy M. Harrison^{1,11}, and Manuel Dall'Osto¹⁰

¹School of Geography, Earth, and Environmental Sciences, University of Birmingham, Edgbaston Rd, Birmingham, B15 2TT, United Kingdom

²Finnish Meteorological Institute, 00101 Helsinki, Finland

³Institute for Atmospheric and Earth System Research, University of Helsinki, 00014 Helsinki, Finland

⁴British Antarctic Survey, NERC, High Cross, Madingley Rd, Cambridge, CB3 0ET, United Kingdom

⁵Institute of Polar Science (IPS), National Research Council (CNR), Venice, Italy

⁶Korea Polar Research Institute, 26, SongdoMirae-ro, Yeonsu-Gu, Incheon, 406-840, Korea

⁷Alfred Wegener Institute (AWI), Helmholtz Centre for Polar and Marine Research, Bremerhaven, Germany

⁸Servicio Meteorológico Nacional (SMN), Av. Dorrego 4019, Buenos Aires, Argentina

⁹Consejo Nacional de Investigaciones Científicas y Técnicas (CONICET), Buenos Aires, Argentina

¹⁰Institute of Marine Sciences, CSIC, 08003, Barcelona, Spain

¹¹Department of Environmental Sciences, Faculty of Meteorology, Environment and Arid Land Agriculture, King Abdulaziz University, Jeddah 21589, Saudi Arabia

Correspondence: Manuel Dall'Osto (dallosto@icm.csic.es)

Received: 1 April 2024 – Discussion started: 6 May 2024

Revised: 10 September 2024 – Accepted: 14 October 2024 – Published: 28 January 2025

Abstract. In order to reduce the uncertainty of aerosol radiative forcing in global climate models, we need to better understand natural aerosol sources which are important to constrain the current and pre-industrial climate. Here, we analyse particle number size distributions (PNSDs) collected during a year (2015) across four coastal and inland Antarctic research bases (Halley, Marambio, Dome C and King Sejong). We utilise *k*-means cluster analysis to separate the PNSD data into six main categories. “Nucleation” and “bursting” PNSDs occur 28 %–48 % of the time between sites, most commonly at the coastal sites of Marambio and King Sejong where air masses mostly come from the west and travel over extensive regions of sea ice, marginal ice and open ocean and likely arise from new particle formation. “Aitken high”, “Aitken low” and “bimodal” PNSDs occur 37 %–68 % of the time, most commonly at Dome C on the Antarctic Plateau, and likely arise from atmospheric transport and ageing from aerosol originating likely in both the coastal boundary layer and free troposphere. “Pristine” PNSDs with low aerosol concentrations occur 12 %–45 % of the time, most commonly at Halley, located at low altitudes and far from the coastal melting ice and influenced by air masses from the west. Not only the sea spray primary aerosols and gas to particle secondary aerosol sources, but also the different air masses impacting the research stations should be kept in mind when deliberating upon different aerosol precursor sources across research stations. We infer that both primary and secondary components from pelagic and sympagic regions strongly contribute to the annual seasonal cycle of Antarctic aerosols. Our simultaneous aerosol measurements stress the importance of the variation in atmospheric biogeochemistry across the Antarctic region.

1 Introduction

The pristine region of the Southern Ocean plays a major role in modulating Earth's climate (Carslaw et al., 2013), and natural aerosols are one of the greatest sources of uncertainty in estimates of global radiative forcing (Reddington et al., 2017). This uncertainty becomes greater in polar regions (Carslaw et al., 2013). Aerosols modulate the climate both directly, by absorbing and reflecting radiation, and indirectly, by acting as cloud condensation nuclei (CCN), modulating cloud properties. The surface of the Southern Ocean near the Antarctic continent goes through an annual freezing cycle; this large frozen area harbours one of the globe's largest ecosystems providing a stable habitat for diverse microbial assemblages (Arrigo et al., 2009, 2015). Understanding these processes is key in polar environments where warming processes are rapidly affecting delicate ecosystems (Clem et al., 2020). For example, the Antarctic Peninsula has shown some of the largest increases in near-surface air temperature measured globally across the last 50 years (Turner et al., 2005). The study of the Antarctic environment can also provide an insight into natural pre-industrial aerosol processes and allows us to further our understanding of the pre-industrial baseline (Hamilton et al., 2014).

Antarctic sea ice covers between 1 % (summer) and 5 % (winter) of the global ocean. Antarctic terrestrial productivity and biodiversity occur almost exclusively in ice-free areas that cover less than 1 % of the continent. In Antarctica the coastline extends for 17 968 km and comprises about $34.8\text{--}36.4 \times 10^6 \text{ km}^2$, where 80 % of this surface is covered by ice, even in summer (Peck, 2018; Ronowicz et al., 2019). Overall, there is about 390 071 km² of coast shallower than 200 m (Peck, 2018). Antarctic coastal systems harbour a high diversity of marine and terrestrial ecosystems including Antarctic seaweeds (benthonic macroalgae) and bird colonies (mainly penguins). Antarctic seaweeds (often called macroalgae) are found in shallow (< 200 m), coastal, rocky shores and can cover more than 80 % of the benthic surface (Amsler et al., 2005; Wiencke and Amsler, 2012). The Antarctic and sub-Antarctic region is home for about half of the total worldwide seabird population (Otero et al., 2018). Penguins represent a high proportion of the avian biomass, and their fecal material is one of the main source of phosphorus and nitrogen, representing about 80 % of these elements in the Antarctic marine environment. Seabird colonies also represent a significant source of atmospheric ammonia (NH₃) in remote maritime systems (Riddick et al., 2012; Schmale et al., 2013). These emissions are environmentally relevant as they primarily occur as “hot spots” in otherwise pristine environments.

The role of aerosols in the Antarctic is poorly understood as their sources are many and varied in a relatively understudied region. Emissions from the Southern Ocean and the Antarctic region are characterised by multiple environmental systems including open-ocean water, sea-ice regions and

land, either snow-covered or snow-free. These regions are being affected by our changing climate (Chen et al., 2009). It has long been known that there is a strong seasonal cycle of Antarctic particle number concentrations (Shaw, 1988), leading to the inference that most of the Antarctic aerosol concentration is linked with biological processes occurring in the surrounding oceans. It has been proposed that a large “pulse” over summer months arises from the upper Antarctic plateau (Ito, 1993; James, 1989), although particle number concentrations are much higher in coastal Antarctica. In other words, it is still debatable if the aerosols originate in the upper troposphere, being transported by the Antarctic drainage flow (James, 1989) to the coast by katabatic winds (Ito, 1993; Koponen et al., 2002; Fiebig et al., 2014; Hara et al., 2011; Järvinen et al., 2013; Humphries et al., 2015), or if the marine pelagic (ice-free) and sympagic (ice-containing) boundary layers are a source of ultrafine particles (Herenz et al., 2019; Weller et al., 2011, 2015, 2018; Dall'Osto et al., 2017a; Heintzenberg et al., 2000, 2023).

The Antarctic aerosol summer maximum concentrations (mainly ultrafine particles, < 100 nm) may be largely explained by new particle formation (NPF) events, as reviewed by Kerminen et al. (2018). Super-micrometre aerosols (> 1 µm) will mostly arise from primary sea spray (O'Dowd et al., 1997a, b; Rankin and Wolff, 2003). The accumulation mode (100 nm–1 µm) is a complex intermediary region with both primary and secondary sources related by their multitude of sources and long atmospheric lifetimes (Fossum et al., 2018; Gras and Keywood, 2017). The relative importance of these sources undergoes seasonal cycles related to meteorology and biological productivity.

During the austral summer the concentration of dimethylsulfide (DMS, a trace gas produced by marine plankton) in the water of the Southern Ocean is the highest of the planet (Lana et al., 2011), with high fluxes into the atmosphere, potentially producing high concentrations of sulfuric acid and methanesulfonic acid. However, under typical boundary layer conditions the concentration of sulfuric acid is too low to form particles alone, and another molecule, such as ammonia, is required to stabilise the nucleating clusters (Kirkby et al., 2011). Jokinen et al. (2018) reported the first molecular characterisation of NPF from Aboa Research Station in Antarctica, showing that new particles are formed via clustering of sulfuric acid and ammonia (Kirby et al., 2011). Sources of ammonia and alkylamines are related to animals, mainly birds and seal colonies, and melting sea ice, but the relative importance of each source is unknown (Riddick et al., 2012; Schmale et al., 2013; Brean et al., 2021; Quélever et al., 2022). Iodine oxoacids are also capable of efficiently forming new particles (Baccarini et al., 2020; He et al., 2021; Sipilä et al., 2016), with iodous acid being able to efficiently stabilise clusters of iodic and sulfuric acid, even in the absence of ammonia (He et al., 2023), with modelling studies showing high gas-phase iodine concentrations across Antarctica (Saiz-Lopez et al., 2007). Further, the for-

mation of marine primary aerosol particles and of gas-to-particle precursors is influenced by the uppermost layer of the ocean, the so-called sea surface microlayer (SML) (Cunliffe et al., 2013). The SML – with physicochemical characteristics different from those of subsurface waters (SSWs) – results in dense and active viral and microbial communities (Vaqué et al., 2021; Heinrichs et al., 2024). The microlayer of the ocean is a source of oxygenated volatile organic compounds (VOCs) in the Arctic leading to secondary aerosol formation (Mungall et al., 2017), and it is also likely a source in the Southern Ocean too, although no measurements of this type are available. Therefore, while the limited number of measurement studies implicate sulfuric acid and nitrogenous bases as the drivers of NPF, iodine and VOCs may play a substantial role.

The roles of secondary aerosols produced from biogenic sulfur mainly derived from the atmospheric oxidation of DMS and primary sea-spray aerosols in regulating cloudiness above the Southern Ocean are still a matter of debate (Meskhidze and Nenes, 2006; Korhonen, 2008; Asmi et al., 2010; Quinn and Bates, 2011; Fossum et al., 2018; Lachlan-Cope et al., 2020). The seasonal cycle of primary and secondary aerosol emissions from the Southern Ocean also affects light scattering by aerosols over all Antarctica, including the upper plateau (Virkkula et al., 2022). A recent intensification in Antarctic aerosol measurement field campaigns is revealing that aerosol chemistry in the higher latitudes of Antarctica can be much more complex than two broad natural sources governing the aerosol populations: sea spray (primary, mostly composed of sea salt) and non-sea-salt sulfate (nssSO_4^{2-} , secondary). For example, Paglione et al. (2024) stressed that various not yet fully understood sources and aerosol processes are controlling the Antarctic aerosol primary and secondary populations, with the emissions from sympagic and pelagic ecosystems affecting the variability in submicron aerosol composition both in maritime areas and in the inner-Antarctic regions.

McCoy et al. (2015) suggested that primary marine organic ultrafine aerosols are important in the Southern Ocean region. Saliba et al. (2021) found that the large total organic fraction of particles $< 0.1 \mu\text{m}$ diameter may have important implications for CCN number concentrations and indirect radiative forcing over the Southern Ocean. Recently, Humphries et al. (2021) identified three main aerosol sources in the Southern Ocean: northern ($40\text{--}45^\circ\text{S}$), mid-latitude ($45\text{--}65^\circ\text{S}$) and southern ($65\text{--}70^\circ\text{S}$) sectors, with different mixtures of continental and anthropogenic, primary and secondary aerosols depending on the studied region.

Recently, several long-term measurements (on the order of a year or longer) of aerosol particle number size distributions (PNSDs) at a high time resolution allow the investigation of the aerosol sources around the Antarctic continent. The PNSD is typically measured from $\sim 10\text{--}1000 \text{ nm}$, and in Antarctica it is usually comprised of particles from sec-

ondary (NPF) and primary (blowing snow – BS; sea-spray aerosols – SSAs) sources.

At King Sejong Station on the Antarctic Peninsula (Kim et al., 2017; Park et al., 2023; Kim et al., 2019), Halley on the mainland coast (Lachlan-Cope et al., 2020) and Dome C (Concordia) in the centre of the continent (Järvinen et al., 2013), PNSD measurements indicated NPF as a mostly summertime phenomenon. At Dome C weak and rare but real NPF has been observed even in June, the darkest time of the year (Järvinen et al., 2013). Particle counts and CCN numbers at Macquarie Island and throughout the Southern Ocean undergo a summertime maximum (Humphries et al., 2023). The CCN concentration at the onset of NPF showed an average instantaneous increase of 44 % or 11 % across the whole period compared with the background concentration (Kim et al., 2019; Park et al., 2023). NPF therefore seems to modulate particle and CCN counts in the Antarctic.

At Halley, NPF events were shown to arise both from the sea-ice marginal zone and the Antarctic plateau, indicating a marine and free-tropospheric source (Lachlan-Cope et al., 2020). NPF events at King Sejong Station were found to be more frequently associated with air masses originating from the Bellingshausen Sea than those from the Weddell Sea, with a fraction of events being associated with sea ice (Park et al., 2023). This suggests the phytoplankton composition of the Bellingshausen Sea may be a source of NPF precursors (Jang et al., 2019). In Marambio, Quéléver et al. (2022) reported neutral and charged aerosol precursor molecules and clusters, as well as charged and neutral PNSDs. NPF precursors were inferred to be related to local fauna (mainly penguins) and oceanic emissions from the Bellingshausen Sea.

Hara et al. (2021) hypothesised that NPF mainly occurred in the Antarctic free troposphere during spring and autumn and in both the free troposphere and boundary layer during summer, based on PNSD measurements and their effect on cloud properties observed at Syowa Station. Dome C's observations reported the background PNSD had its largest mode below 30 nm, suggesting these particles were produced in the upper atmosphere before entering continental Antarctica (Järvinen et al., 2013). However, also ground-level particle formation takes place on the upper plateau. Chen et al. (2017) reported NPF events that were observed at Dome C by using a combination of an air ion spectrometer (AIS) and a differential mobility particle sizer (DMPS). In several events particle formation and growth started from the cluster ion size range of 0.9–1.9 nm, which means that in these cases the formation took place at the ground level; however, NPF precursor emissions from the plateau itself are believed to be negligible, implying they are transported from elsewhere. NPF in Antarctica is therefore dependent on biogenic emissions from the ice-covered and ice-free regions of the ocean, with NPF occurring both at ground level and in the colder upper atmosphere where particle formation rates can proceed more rapidly.

Table 1. Latitude and longitude of each site.

Site	Lat	Long	Elevation a.s.l. (m)
King Sejong	−62.2	−58.8	10
Marambio	−64.2	−56.6	198
Dome C	−75.1	123.3	3233
Halley	−75.6	−26.2	30

Previous analyses of PNSDs at Halley using *k*-means cluster analysis has shown that wintertime PNSDs were characterised by extremely low particle concentrations, with a bimodal PNSD appearing with a blowing-snow or sea-spray origin (Lachlan-Cope et al., 2020). The Antarctic wintertime at this site is therefore mostly devoid of secondary aerosol sources and is instead dominated by primary sources. Some of these primary aerosols will be organic, and NMR analyses of ambient aerosol samples show that aerosols arising from the ice-free Southern Ocean are rich in lipids and sugars, and aerosols arising from coastal areas are rich in sugars associated with plant vegetation (Decesari et al., 2020). These sources are likely primary, and the primary aerosol sources are therefore many and varied across Antarctica.

Here, we apply *k*-means cluster analysis to simultaneous measurements in the year 2015 at four Antarctic research sites, extending the study of Lachlan-Cope et al. (2020). We also compare the yearly data with field studies, including the PEGASO (Plankton-derived Emissions of trace Gases and Aerosols in the Southern Ocean) cruise in 2015 (Dall’Osto et al., 2017a, 2019b; Rinaldi et al., 2020; Decesari et al., 2020) and the continental Antarctic site Kohnen (Weller et al., 2018). We show a prevalence of new particle formation at the coastal sites and associate this new particle formation with air masses flowing over regions of sea ice and ocean. At the more southerly and inland sites, primary particles dominate the particle number concentrations, while air masses primarily travel over regions of land. Ambiguity remains in this analysis, as some PNSD clusters likely contain a substantial contribution from primary and secondary processes. Nonetheless, we provide further evidence for the roles of emissions from sympagic and pelagic ocean regions in new particle formation and highlight the many and varied sources of particles across Antarctica.

2 Methodology

2.1 Sampling sites and measurements

Simultaneous PNSD measurements at four sites across Antarctica were collected for analysis. Their locations are stated in Table 1 and shown in Fig. 1. Data coverage is shown in Fig. S1 in the Supplement. PNSD measurements were aggregated to 1 h for this study.

The South Korean King Sejong Station, the highest-latitude site, is located on the Antarctic Peninsula. The PNSD from 10 to 300 nm was measured every 3 min with a mobility particle size spectrometer (MPSS) consisting of a differential mobility analyser (DMA; HCT, Inc., LDMA 4210) and a condensation particle counter (CPC; TSI 3772). Details of the site can be found in Kim et al. (2017, 2019) and Park et al. (2023).

The Argentinian Marambio Station is located on the Antarctic Peninsula, approximately 3 km from the coast. The PNSD from 12–800 nm was measured every 6 min with a differential MPSS (Asmi et al., 2010; Quéléver et al., 2022).

The French- and Italian-operated Dome C station is operated on the eastern Antarctic Plateau at an elevation of > 3000 m a.s.l and height of 900 km from the nearest coast. The Dome C sampling site is located 1 km southwest of Dome C’s main building. The PNSD from 10–620 nm was measured every 10 min with a differential MPSS system (Järvinen et al., 2013).

The British Halley VI station is located in coastal mainland Antarctica on the floating Brunt Ice Shelf ~ 20 km from the coast of the Weddell Sea. The Clean Air Sector Laboratory where PNSD measurements are taken is located 1 km southeast of the station. The PNSD from 6 to 209 nm was measured every 1 min using a TSI Inc. MPSS, comprising an electrostatic classifier (model 3082), a condensation particle counter (CPC; model 3775) and a long differential mobility analyser (DMA; model 3081) (Lachlan-Cope et al., 2020).

2.2 Data processing

A *k*-means cluster analysis was applied to the PNSD data to apportion the PNSDs according to their shape (Beddows et al., 2009), and this is routinely applied in pristine environments to PNSD data (Dall’Osto et al., 2017b, 2019b; Lachlan-Cope et al., 2020), including the Halley dataset used in this paper (Lachlan-Cope et al., 2020). The *k*-means analysis apportions data into *k* clusters such that the sum of squares of distances of data to the cluster centre is minimised. In the case of MPSS data, this produces well-separated clusters (Beddows et al., 2009). First, data were normalised so the Euclidian length of each PNSD was 1, so the clustering is done solely on the merit of the shape of the PNSDs. Here, a degree of distance between clusters was achieved with 16 MPSS clusters. These were assigned into six categories typical of Antarctic PNSDs (Lachlan-Cope et al., 2020). Compared to previous work, we combined the three “pristine” clusters identified by Lachlan-Cope et al. (2020) into one, as they follow the same seasonal trend, producing six clusters instead of eight.

The condensation sink (CS, s^{-1}) represents the rate at which a vapour-phase molecule will collide with a pre-existing particle surface and was calculated from the PNSD

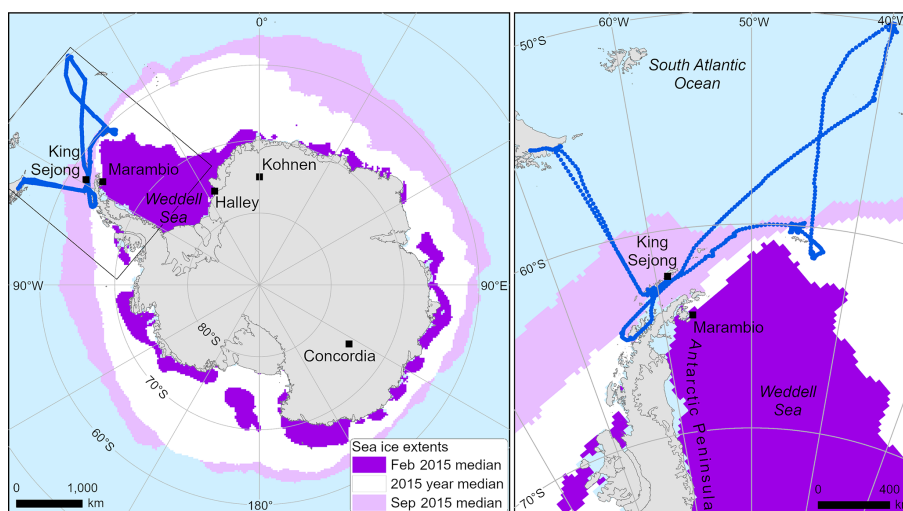


Figure 1. Map of the sampling stations (Halley, Marambio, Dome C, King Sejong) for the dataset collected in 2015. Additional data for shorter period are intercompared at Kohlen (Weller et al., 2018) and during the PEGASO cruise (Dall’Osto et al., 2017a; blue line is the PEGASO cruise track). The February sea-ice extent signifies the annual minimum, while the September median signifies the annual maximum (data are from the National Snow and Ice Data Center – NSIDC – at <https://nsidc.org/data/>, last access: 30 July 2024, Fetterer et al., 2017).

data as follows (Kulmala et al., 2012):

$$CS = 2\pi D \sum_{d_p} \beta_{m,d_p} d_p N_{d_p}. \quad (1)$$

Here, D represents the diffusion coefficient of the condensing vapour, which is assumed to be sulfuric acid. The transitional regime correction factor is denoted by β_{m,d_p} , d_p is the diameter of a measurement bin, and N_{d_p} is the number of particles in size bin d_p .

2.3 Air mass trajectories

Air mass back trajectories were calculated using the HYSPLIT (Hybrid Single Particle Lagrangian Integrated Trajectory) trajectory model (Draxler and Rolph, 2010) arriving at the sampling site every 1 h. Each back-trajectory data point was assigned to a surface type (land, sea, ice or snow over land; a cell is considered ice-covered if more than 40 % of the cell is covered with ice) on a 24 km grid from the daily Interactive Multisensor Snow and Ice Mapping System (IMS) (U.S. National Ice Center, 2008). To investigate air masses concurrent with high particle count, these 72 h back trajectories were gridded to 1×1 grid cells of 1° each and linked back to the total integrated particle number concentration from the PNSD measurements by the following equation:

$$\ln(\bar{C}_{ij}) = \frac{1}{\sum_{k=1}^N \tau_{ijk}} \sum_{k=1}^N \ln(c_k) \tau_{ijk}, \quad (2)$$

where \bar{C}_{ij} is the concentration-weighted trajectory (CWT) at cell i, j , N is the total number of trajectories, c_k is the value of particle number (N) associated with the arrival of

trajectory k , and τ_{ijk} is the residence time of trajectory k in grid cell i, j . \bar{C}_{ij} therefore describes the source strength of condensable vapour that drives particle growth from any particular grid cell (Hsu et al., 2003; Lupu and Maenhaut, 2002). This was done using the `trajLevel` function in the `openair` package in R 3.6.3.

3 Results

3.1 Trends in aerosol PNSDs

The mean PNSDs for the measured periods are shown in Fig. 2a. PNSDs at the two Antarctic Peninsula sites, Marambio and King Sejong, show large nucleation modes. Aitken mode peaks are present at all sites with maximum concentrations between 30 and 50 nm. Accumulation mode peaks are present at all sites with maximum concentrations > 100 nm. The prominent nucleation modes at Marambio and King Sejong are also visible in the daily contour plots, with the visible signature of a new nucleation mode in the late and early afternoons (local times) at the two sites, respectively (Fig. S3). Total average particle counts are highest at King Sejong and Marambio (312 ± 601 and $270 \pm 541 \text{ cm}^{-3}$), and particle counts at Halley are lower ($223 \pm 245 \text{ cm}^{-3}$), while those at Dome C are $44 \pm 67 \text{ cm}^{-3}$.

The monthly variation in total particle number (N_{tot}) is similar between all sites and highest in the austral summer, with minimum values in July and August. N_{tot} at Dome C is substantially lower in nearly all months compared to all other sites, with the monthly average only exceeding 100 cm^{-3} in the austral summer months (November, December). Relative contributions of the modes < 30 , 30–100 and > 100 nm

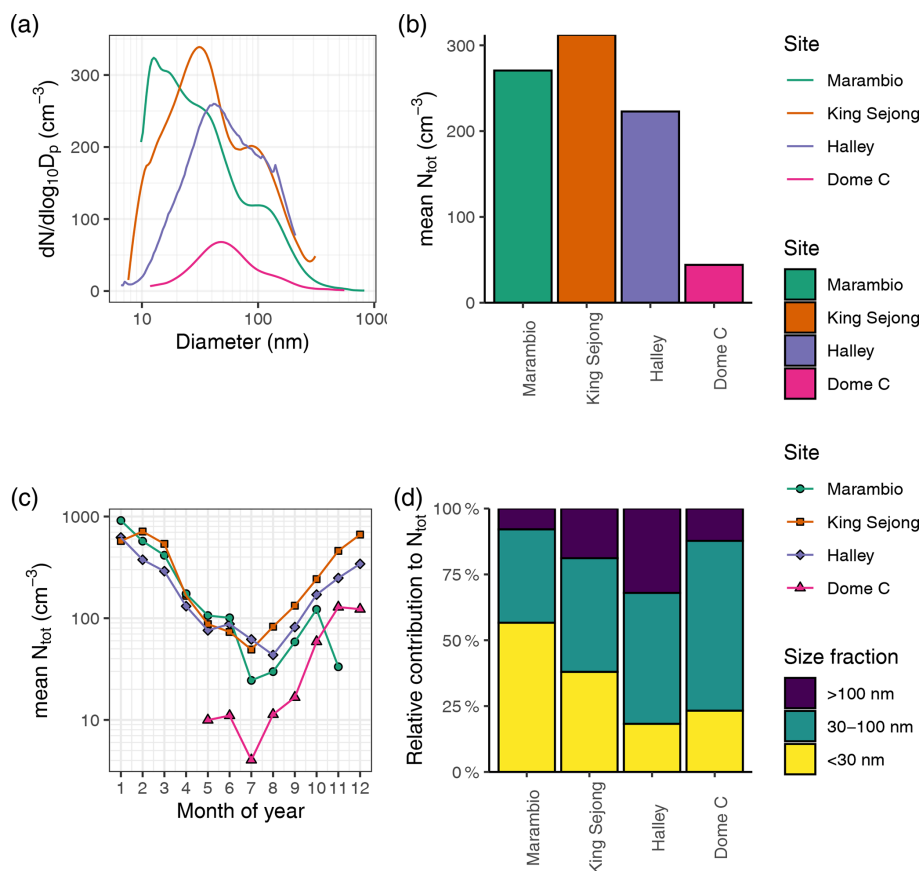


Figure 2. Features of particle PNSD data for four Antarctic sites, showing (a) mean particle PNSD per site, (b) mean particle count per site, (c) seasonal variation in particle count per site and (d) contribution of different size fractions to particle count per site. Only data from the same time period (April–December) are intercompared and presented in panels (a), (b) and (d), whereas the whole temporal trend is presented in panel (c).

to N_{tot} at each site are shown in Fig. 2d. The relative contribution of < 30 nm particles is highest at Marambio and King Sejong, exceeding 50% of the total N_{tot} at Marambio, consistent with the prominence of the presence of the nucleation mode (Fig. 2a). The contribution of < 30 nm particles to total N_{tot} is lowest at Halley, where $\sim 50\%$ of the N_{tot} comes from the mode 30–100 nm and $\sim 30\%$ from the mode > 100 nm. At Dome C, $\sim 65\%$ of N_{tot} comes from the mode 30–100 nm, with small contributions from particles above or below this size range.

3.2 Cluster analysis

3.2.1 Categorising PNSD k -means clusters

A k -means cluster analysis was used to partition the PNSD data into days with similarly shaped PNSD data. In k -means cluster analysis, starting with a higher number of clusters and then merging them based on similarity can enhance the separation and interpretability of the final clusters by capturing finer details. These 16 daily k -means clusters (Fig. S2, referred to onwards as the initial PNSD clusters) were therefore

aggregated into 6 daily categories typical of Antarctic PNSD data (referred to as simply the PNSD clusters) for further analysis based on the shape of the PNSD and their temporal variation (Fig. 3a and b). These are nucleation, bursting, Aitken high, Aitken low, pristine and bimodal, following previous classifications described in previous studies (Dall’Osto et al., 2017b, 2019b; Lachlan-Cope et al., 2020). The diurnal cycle of the PNSD belonging to each of the initial 16 k -means clusters at each of these sites is shown in Fig. S4, while the diurnal cycle of the merged clusters is shown in Fig. S5, separated by site, and the PNSD per cluster separate by season is shown in Fig. S6.

Two clusters relate to NPF: nucleation (mean particle count $502 \pm 1087 \text{ cm}^{-3}$) has a mean PNSD with a peak at 12 nm averaged between all sites. This corresponds to fresh new particles generated during NPF events and will correspond to days of measurements dominated by a signature of new particles appearing in the PNSD, typically with signs of growth. Bursting (mean particle count $177 \pm 350 \text{ cm}^{-3}$) has a mean PNSD with a peak at 22 nm averaged between all sites and typically corresponds to days when new particles

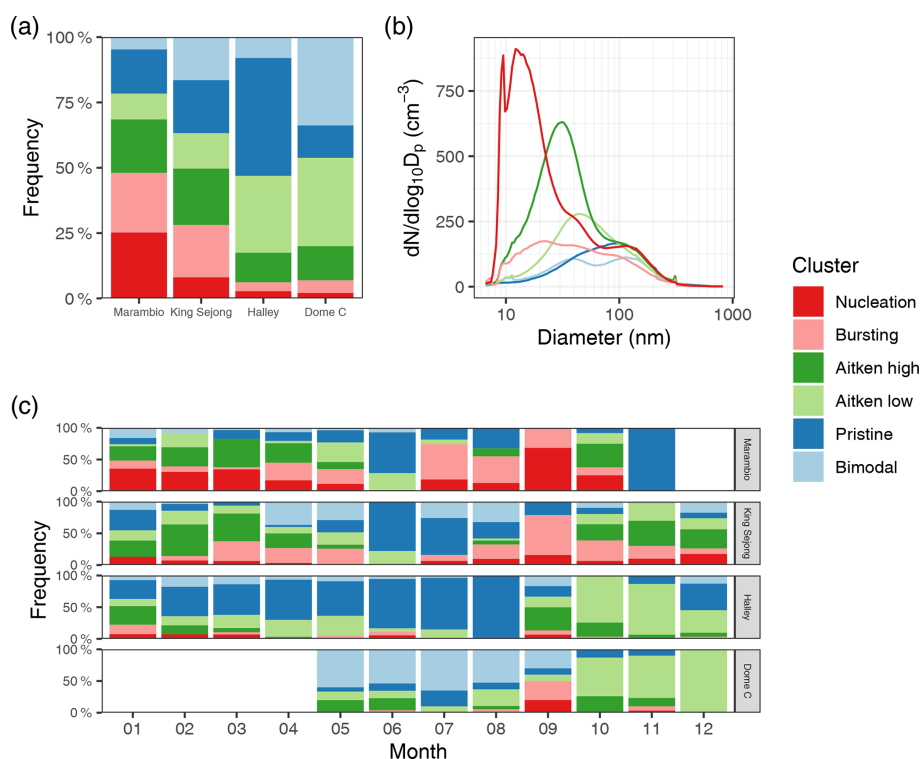


Figure 3. Cluster analysis results, showing (a) average frequency of each cluster per site, (b) mean PNSD per cluster and (c) seasonal variations in cluster frequency per site.

form or either fail to grow, are lost to coagulation, or are diluted and lost before arrival at the receptor site. Note that the name “bursting” refers to “bursts” in particle number concentrations due to secondary formation, rather than bubble bursting. These likely still do correspond to secondary formation processes. We presume here that there is no primary contribution to these PNSDs.

Aitken is the most common PNSD category separated into Aitken high (mean particle count $401.6 \pm 45.5 \text{ cm}^{-3}$) and Aitken low (mean particle count $208.8 \pm 216.7 \text{ cm}^{-3}$). The mean PNSD shows peak concentrations at about 20–35 and 35–55 nm, respectively. These two clusters are separated based on their aerosol total concentrations. The name of this category emerges from growing ultrafine aerosol resulting from the processing of local and regional marine aerosols, a phenomenon previously described as occurring mainly in summer (Dall’Osto et al., 2017b).

Pristine (mean particle count $142 \pm 134 \text{ cm}^{-3}$) has a mean PNSD with a peak at 88 nm. The name of this category emerges from the extremely low “pristine” particle number concentrations. The three *k*-means clusters belonging to this category have some specific aerosol modes, peaking at 65 nm, 85 nm and a much larger accumulation mode at 160 nm (Fig. S2) likely associated under pristine conditions with high loadings of blowing snow, as previously discussed in Lachlan-Cope et al. (2020).

Bimodal (mean particle count $107 \pm 133 \text{ cm}^{-3}$) has two peaks in the PNSD at 39 and 113 nm. Both are characterised by low particle counts. The name of this category is associated with the bimodal PNSD. The two initial clusters differ slightly because of the Hoppel minimum at 55 and 75 nm, respectively; the Hoppel minimum refers to a specific dip in the number concentration of aerosol particles at these sizes, suggesting variations in particle stability, growth or origin.

The condensation sink represents the main loss process for many low-volatility vapours which contribute to new particle formation. The condensation sink for the bursting *k*-means cluster is lowest ($2.3 \times 10^{-4} \text{ s}^{-1}$), followed by bimodal ($2.4 \times 10^{-4} \text{ s}^{-1}$), pristine ($3.4 \times 10^{-4} \text{ s}^{-1}$), nucleation ($3.7 \times 10^{-4} \text{ s}^{-1}$), Aitken low ($3.4 \times 10^{-4} \text{ s}^{-1}$) and Aitken high ($4.0 \times 10^{-4} \text{ s}^{-1}$). Particle counts change by around 1 order of magnitude between sites, but the shapes of the PNSD are similar (Figs. S2, S5). All nucleation PNSDs show the formation and growth of particles at midday and afternoon times (local time), while bursting shows particles at or near the smallest sizes, sometimes with an indication of particle growth (Figs. S4, S5).

3.2.2 Trends in PNSD *k*-means clusters

The frequency of occurrence of these different PNSD clusters can indicate the dominant sources of aerosol particles at each of these time periods. All sites have a large contribu-

tion from Aitken low and Aitken high PNSD clusters, with 37 % of PNSDs falling into these categories across all four sites. Marambio is also dominated by PNSD clusters falling into the nucleation and bursting category (25 % and 23 % of PNSDs, respectively). There is a smaller contribution of nucleation and bursting to the PNSDs at King Sejong (8 % and 20 %, respectively). These PNSD clusters contribute little at Halley (3 % and 3 %, respectively) and at Dome C (2 % and 5 %, respectively). Halley instead sees a large contribution of pristine PNSDs (45 % of PNSDs), and Dome C sees a large contribution of bimodal PNSDs (34 % of PNSDs) (Fig. 3a).

The seasonal evolution of these *k*-means clusters is shown in Fig. 3c. At Marambio, the contribution of nucleation and bursting PNSDs occurs in nearly all months. At King Sejong, nucleation and bursting PNSDs are most frequent in the spring and autumn months, while pristine air masses are most common in the austral winter. At Halley, Aitken PNSDs dominate the warmer months, while pristine air masses dominate the colder winter months. At Dome C, where data are available, bimodal PNSDs dominate the winter, while Aitken dominates the warmer months. There is a substantial contribution of nucleation and bursting in the month of September also. When all sites are averaged, a clear seasonal cycle is seen, with pristine and bimodal PNSDs dominating in the coldest months and a substantial contribution of Aitken in the warmer months. Nucleation is slightly higher in the warmer months (particularly January through March), while bursting PNSDs are higher outside of these months.

3.3 Air mass analysis

The 72 h HYSPLIT back trajectories arriving at the four different measurement sites for every hour with PNSD data were calculated. The amount of time each of these air masses spent flowing over land, open ocean, marginal ice or sea ice per *k*-means cluster across all sites is plotted in Fig. 4a and per site is plotted in Fig. 4b. On average, the air masses arriving at the sites had flown over most of the land of the Antarctic continent (54 %), with a 24 % contribution from sea ice, 15 % contribution from open water and a small (6 %) contribution from marginal ice. Nucleation and bursting PNSDs occur when air masses have travelled over substantially less land and over more sea ice, marginal ice and ocean than average (40 %, 8 % and 26 % of air mass hours for nucleation and 34 %, 10 % and 25 % of air mass hours for bursting, respectively). At Marambio, the main contribution is air masses arising from sea-ice regions (50 %), which is highest for bimodal PNSDs (76 %). The contribution of open water to Aitken, bursting and nucleation is higher than average (23 %), while the contribution of sea ice to these air masses is lower (44 %). At King Sejong, air masses spend the majority of their time travelling over regions of open water (41 %) and sea ice (33 %). The contribution of open water is higher for bimodal (51 %) and Aitken PNSDs (58 %). At Halley, air masses spend the majority of their time flowing over land re-

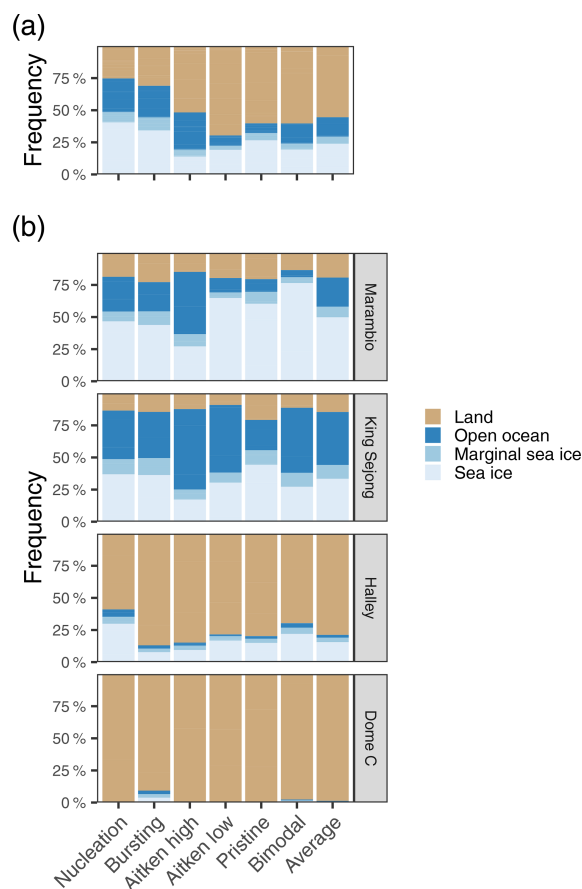


Figure 4. Land surface types associated with each cluster, showing (a) average association across all sites and (b) association per site. “Average” is the mean of all clusters.

gions (79 %), with a small contribution from sea ice (15 %). The contribution of sea ice to nucleation PNSDs is substantially higher (30 %). At Dome C, air masses arriving at the receptor site mostly flow over land (99 %). The contributions of sea ice, marginal ice and open water are higher for bursting PNSDs (9 % in total).

Our CWT analysis grids back trajectories to $1^\circ \times 1^\circ$ squares and weighs each segment of the back trajectory with the corresponding N_{tot} observed upon the air mass’s arrival, performed individually for each PNSD cluster. These are plotted in Fig. 5. A map highlighting source regions for N_{tot} unseparated by cluster per site is shown in Fig. S8. The CWTs aggregated together for each site are shown in Fig. S9. Mean heights of these trajectories are shown in Fig. S10.

The sources of particles by number (or, N_{tot}) across all PNSD data at the two Antarctic Peninsula sites, Marambio and King Sejong, are to the west of the peninsula, across the iced and open-water regions of the Bellingshausen Sea and to a lesser extent the Weddell Sea. Those at Halley are concentrated at the coastal and land-based regions, with some influence from the Weddell Sea, while the highest aerosol

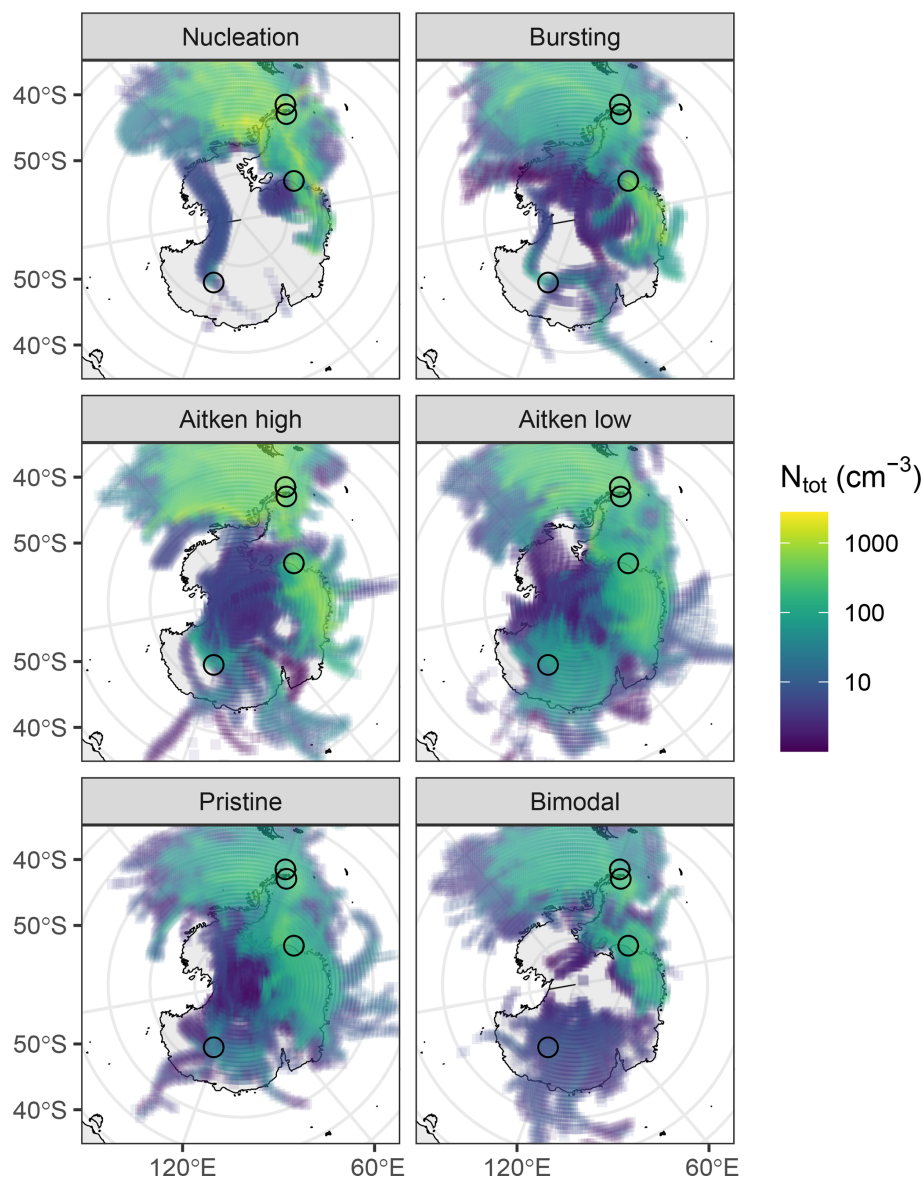


Figure 5. Concentration-weighted trajectory maps showing the sources of particles corresponding to each cluster at each site. The 72 h back trajectories are calculated with HYSPLIT.

concentrations at Dome C arise from mostly land regions, with some trajectories extending past the southern tip of the continent over ocean regions (Fig. S8).

Air masses arriving at the Antarctic sites corresponding to nucleation and bursting *k*-means clusters pass mostly over the Bellingshausen Sea at Marambio and King Sejong. Air masses passing over the regions just west of the peninsula have a high source contribution to high number concentrations of particles especially, as do the more northerly regions off the southern tip of South America. At Halley, these PNSD clusters are mostly associated with coastal regions, consistent with the higher contribution of sea ice. The source contributions at Dome C correspond to a small number of trajec-

tories. All trajectories corresponding to nucleation PNSDs have a lower-than-average trajectory height, although the total number of trajectories this corresponds to is relatively small (Fig. S10).

Aitken PNSDs have strong source contributions from the entire Bellingshausen Sea region at Marambio and King Sejong. At Halley, there is a strong contribution from land mass regions, while at Dome C, land regions contribute to this PNSD. Bimodal and pristine air masses at Marambio and King Sejong have strong source contributions from the iced regions either side of the Antarctic Peninsula, covering the Weddell and Bellingshausen seas. This is consistent with the higher contribution from sea-ice regions to these *k*-

means clusters. At Halley, the bimodal PNSDs arise when air masses flow over coastal and land-based regions, while pristine PNSDs, which are extremely frequent at this site, arise largely from the Antarctic continent itself. At Dome C, there is a strong source contribution to bimodal and pristine PNSDs from air masses flowing over the coastal region of southern Antarctica, as well as some land regions. Trajectories corresponding to pristine PNSDs have, on average, a higher trajectory height than average.

3.4 Intercomparison with other existing data across the year 2015

3.4.1 PEGASO cruise

The PEGASO (Plankton-derived Emissions of trace Gases and Aerosols in the Southern Ocean) cruise was conducted on board the RV *Hesperides* in the regions of the Antarctic Peninsula, South Orkney Islands and South Georgia Islands from 2 January to 11 February 2015. It was found that the microbiota of sea ice and the sea-ice-influenced ocean can be a source of atmospheric primary and secondary organic nitrogen (ON), specifically low-molecular-weight alkylamines (Dall'Osto et al., 2017a, 2019a). Other follow-up studies also claim that the potential impact of the sea-ice (sympagic) planktonic ecosystem on aerosol composition was overlooked in past studies, and multiple eco-regions act as distinct aerosol sources around Antarctica (Decesari et al., 2020; Rinaldi et al., 2020).

Figure 6a shows the intercomparison of MPSS PNSDs for the PEGASO cruise. These are separated into times when the air masses flowed over the Pacific Ocean and over the Weddell Sea. This is compared with stations used for this study where overlapping data are available (Marambio, King Sejong and Halley). Air masses from the southern Pacific Ocean with anthropogenic and terrestrial influence from Patagonia are likely responsible for the higher Aitken mode seen for the “Pacific” PNSD during the PEGASO cruise. By contrast, cruise measurements influenced by the Weddell Sea show a PNSD similar to the three stations intercompared, suggesting little anthropogenic influence of the latter. Dall'Osto et al. (2017a) showed that sea-ice regions are a strong source of sub-3 nm particles in Antarctica relative to open-water regions. The present study, considering a much broader dataset, also shows that the open-water regions sampled at Marambio and King Sejong stations are also associated with enhanced NPF.

3.4.2 Kohnen Station

Weller et al. (2018) reported PNSDs and conducted bulk and size-segregated aerosol sampling during two summer campaigns in January 2015 and January 2016 at the continental Antarctic station Kohnen (Dronning Maud Land). The transport of aerosols was associated with two main weather conditions: (1) the sporadic impact of cyclones causing high load-

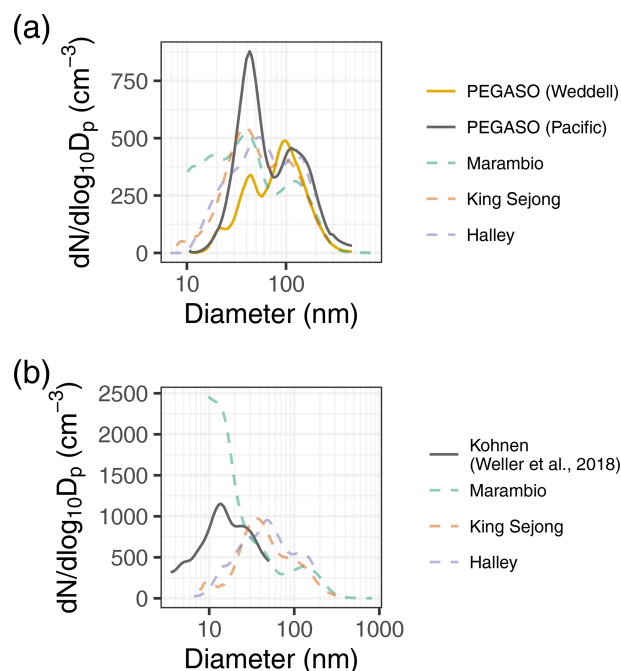


Figure 6. PNSD intercomparisons: (a) PNSD from the PEGASO cruise when influenced from air masses from both the Weddell Sea and Pacific Ocean and the stations used for this study where overlapping data are available (Marambio, Halley and King Sejong stations) and (b) PNSD from Kohnen Station (Weller et al., 2018) and the stations used for this study where overlapping data are available (Marambio, Halley and King Sejong stations).

ings of marine aerosol concentrations and NPF and (2) clear-sky conditions causing long-range transport of aged aerosols. Figure 6b shows similar aerosol PNSDs among Kohnen, Halley and King Sejong stations for the same sampling period in 2015. By contrast, much higher concentrations of ultra-fine particles – likely due to NPF – were seen occurring at Marambio. This may be a combination of local sources (nearby penguin colonies) and melting sea ice during the summer period, given Marambio is the station among them all closest to marginal sea-ice zones (Quéléver et al., 2022).

4 Discussion

4.1 Possible primary sources

Of our six aerosol categories, nucleation and bursting are related to secondary aerosols, while the two Aitken *k*-means clusters likely have significant contributions from primary and secondary processes (Fig. 2a), although the latter may dominate. Bimodal PNSDs are likely associated with aged and processed marine aerosols (the Hoppel minimum mode is seen at about 70 nm; Hoppel et al., 1994). We cannot apportion primary aerosols from our PNSD measurements without any chemical composition information but can hypothesise some. Sea salt aerosol particles are formed from

open ocean regions when sea spray is produced by wave breaking and bubble bursting generating film and jet drops (De Leeuw et al., 2011). Sea salt aerosol is also formed from blowing snow above sea ice (Frey et al., 2020). These mechanisms are thought to contribute equally to sea salt aerosol loads (Legrand et al., 2016), while blowing snow over land is a source from continental Antarctica (Giordano et al., 2018).

In the periods when NPF is negligible, there are still other primary aerosol sources. We show that pristine and bimodal PNSD clusters dominate through the winter (Figs. 3c, S6). It is therefore important to characterise these pristine conditions. The three *k*-means clusters of the pristine categories have similar low particle number concentrations, but one of the three has a distinct PNSD. The cluster (pristine_160), seen with a bimodal PNSD (75 and 160 nm, respectively), was strongly associated with high wind speed and possibly associated with blowing snow and sea-spray sea salt, dominating the winter aerosol population (Lachlan-Cope et al., 2020). When the four stations are compared in this study, it can clearly be seen that Halley has the most frequent pristine conditions (45 %, relative to the 12 %–20 % of the other three), also relative to Dome C where we propose that free-tropospheric transport and aged aerosols populate the PNSD with Aitken modes and bimodal PNSDs.

The pristine initial PNSD cluster with a strong peak at 160 nm (Table S1 in the Supplement) is seen mainly at Halley (12 %) relative to the other stations (2 %–3 %). A study by Yang et al. (2019) proposes a source for ultrafine sea salt aerosol particles from blowing snow, dependent on snow salinity. This mechanism could account for the small particles seen during Antarctic winter at coastal stations (Giordano et al., 2018; Frey et al., 2020). Recently, similar PNSD were reported by Gong et al. (2023) in the central Arctic over an entire year from September 2019 to October 2020 during the Multidisciplinary drifting Observatory for the Study of Arctic Climate (MOSAIC) expedition, showing that blowing snow was observed more than 20 % of the time from November to April. The sublimation of blowing snow generates high concentrations of fine-mode sea salt aerosol (diameter below 300 nm), enhancing cloud condensation nuclei concentrations by up to 10-fold above background levels (Gong et al., 2023).

Primary marine organic aerosol in the submicron regime is likely produced separately from sea salt (Gantt and Meskhidze, 2013). At the coastal sites of Marambio and Halley, bimodal and pristine PNSDs with the highest particle number concentration arise mostly from the Bellingshausen Sea, where DMS(P)-rich phytoplankton concentrations are very high. A dominant biological oceanic mechanism of primary particle origin at these sites is therefore likely. Given the vastly different source characteristics between these sites, it is likely that the dominant mechanisms of origin of these primary particles, and therefore our bimodal and pristine clusters, also differ between sites, but it is clear that primary emissions dominate the PNSD in the Antarctic winter.

4.2 New particle formation and possible secondary sources

We identify two PNSD clusters which we classify as arising from secondary processes: these are nucleation and bursting PNSDs. The Aitken PNSD clusters cannot be definitively said to contain solely particles from secondary processes, although they have similar source regions (Fig. S5) and could consist of grown particles formed either elsewhere in the boundary layer or in the free troposphere, with average growth rates of around $\sim 0.1\text{--}1\text{ nm h}^{-1}$ (Brean et al., 2021; Järvinen et al., 2013; Jokinen et al., 2018; Kim et al., 2019); particles formed through NPF would grow to the sizes observed in this PNSD cluster on the order of $\sim 2\text{ d}$. The contribution of Aitken PNSDs is greatest outside of the winter months (Fig. S7). However, below, we will purely discuss the contribution of the bursting and nucleation PNSDs.

NPF in Antarctica is a summertime phenomenon largely responsible for the seasonal cycle in particle number concentrations (Fig. 2c). This cycle has been observed at King Sejong Station (Kim et al., 2017; Park et al., 2023; Kim et al., 2019), Halley (Lachlan-Cope et al., 2020) and Dome C (Järvinen et al., 2013; Chen et al., 2017). This corresponds with periods of high biological and photochemical activity (Jang et al., 2019; Kim et al., 2019). These observations are consistent with our observed higher frequency of nucleation PNSD clusters in January through March (Figs. 3c, S6). However, we consistently observe nucleation and bursting PNSDs year-round, even at sites where manual inspection of these PNSDs has found little to no NPF in the winter seasons (Kim et al., 2019).

We frequently observe PNSDs with a large nucleation mode in the austral summer (Fig. S7). NPF is mainly influenced by the source rates of vapours, including emissions of dimethylsulfide (DMS), volatile organic compounds (VOCs) and bases such as NH_3 and iodine, as well as OH^\bullet and O_3 production rates, loss rates of vapours and new particles (CS), ion pair production rates, and temperature (Lee et al., 2019). Vapour source rates will be lowest in winter; however, ion pair production from cosmic rays is likely constant, while loss rates of vapours and temperatures have a wintertime maximum. Some number of particles may therefore form and be identified by cluster analysis, even when they do not give the visual signature of an NPF event.

Our analyses show that coastal Antarctic sites nearest to the melting sea ice are most influenced by NPF (Fig. 3c) where a large fraction of the PNSDs are classified as nucleation and bursting (48 % and 28 % at Marambio and King Sejong, respectively). Further, we show that NPF is frequent when air masses flow over the ice-influenced oceanic Antarctic regions (Figs. 4, 5). NPF events have been shown to be frequent and strong at coastal Antarctic sites (Brean et al., 2021; Jokinen et al., 2018) but most rapid at those nearest to melting ice (Brean et al., 2021) as well as near local sources associated with penguin colonies (Quéléver et

al., 2022). Recent observations shows that this does not extend across the whole of the Southern Ocean (Baccarini et al., 2021). Our PNSD cluster analysis is consistent with this. Melting sea is therefore a likely source of NPF precursors in the Antarctic Peninsula region.

High aerosol number concentrations arising from the Bellingshausen Sea are consistent with a previous analysis of NPF at King Sejong (Jang et al., 2019). Bursting and nucleation aerosol categories in particular exhibit high number concentrations when air masses pass over the regions just west of the peninsula (Fig. 5). These regions have been shown to be rich in alkylamines (Dall'Osto et al., 2019a), which leads to rapid and efficient particle formation (Brean et al., 2021). There is evidence that these melting sea-ice regions are sources of numerous NPF precursors (Atkinson et al., 2012; Dall'Osto et al., 2017a, 2019a). This is also consistent in the sympagic Arctic environment (Dall'Osto et al., 2017b, 2018). Consistent with this, the results of our *k*-means cluster analysis show that the sites with the highest exposure to air masses that pass over regions of sea ice and marginal ice have by far the greatest contribution from nucleation and bursting PNSD types (Figs. 2, 4). The sites where air masses primarily travel over snow-covered land regions have, by contrast, very little contribution from nucleation and bursting (Fig. 4a).

The role of new particles formed in the free troposphere and transported down to our receptor sites is unknown but likely. Particle formation processes are highly efficient in the free troposphere given the lower temperatures and higher ion pair production rates. A wider number of potential nucleation mechanisms are therefore likely (Kirkby et al., 2011; Wang et al., 2022). Modelling studies predict a substantial fraction of CCN in all seasons (Korhonen et al., 2008). These particles, if arriving at the receptor site long enough after formation, will contribute to either nucleation, bursting or Aitken PNSDs. While we therefore highlight source regions leading to boundary layer NPF processes, we cannot state what fraction of PNSDs arise from free-tropospheric particle formation processes.

5 Implication and conclusion

Figure 7 shows a schematic illustration of the sea ice, microbiota, sea-to-air emissions, and primary and secondary aerosols in Antarctica. Figure 7 highlights the dominance of NPF in summertime PNSDs and a dominance of primary aerosols during the wintertime, with these primary aerosols being more prevalent inland than at the coast, a key finding of this study. It also highlights the retreat of sea ice in the summer, leading to increased marine emissions, alongside a reduction in terrestrial biological activity and sunlight intensity during winter months.

To gain insight into the influence of marine Antarctic biogeochemistry on atmospheric aerosol, we report simultane-

ous aerosol PNSDs collected across an entire year (2015) at four research stations (Marambio, King Sejong, Halley and Dome C), as well as a brief intercomparison with a cruise around the regions of the Antarctic Peninsula, South Orkney Islands and South Georgia Islands (Dall'Osto et al., 2017a) and a field campaign at Kohnen Station (Weller et al., 2018). Our study shows that the aerosol PNSDs across the Antarctic have striking differences, likely due to multiple eco-regions, and subsequent atmospheric chemical and physical processes act as multiple aerosol sources around Antarctica. These analyses suggest that the PNSD of Antarctic sub-micrometre aerosols may have been oversimplified in the past (Ito, 1993) and that complex interactions between multiple ecosystems, coupled with different atmospheric circulation, result in very different PNSDs populating Antarctica. Our knowledge on aerosol sources of primary and secondary origin is limited.

The Southern Ocean is among the largest sources of sea-spray aerosols (SSAs) on planet Earth. Current aerosol models have a large uncertainty in the SSA abundance (Lapere et al., 2023), and the relative importance of the sublimation of blowing snow is not yet quantified (Giordano et al., 2018; Frey et al., 2020). The biogenic organic component of SSA in Antarctica is thought to be important (McCoy et al., 2015) but again not fully quantified. Sea ice may also modulate SSA production, with potentially significant climate impacts (Dall'Osto et al., 2022a). Other leached material from Antarctic media including seaweeds and penguin guano may also affect cloud-relevant SSA production (Dall'Osto et al., 2022b).

Recently, Brean et al. (2023) emphasised how understanding the geographical variation in surface types across the Arctic is key to understanding secondary aerosol sources, highlighting that particle formation and growth rate vary tremendously, likely due to different regions producing different precursor source rates. The same complexity applies to Antarctica – an ensemble of regions with substantial spatial heterogeneity across marine, terrestrial and freshwater biomes, with productivity and biodiversity patchiness superimposed on strong environmental gradients. Antarctica, one of the world's eight major biogeographical realms, is split into 16 Antarctic Conservation Biogeographic Regions (also known as ecoregions or bioregions; Terauds et al., 2012; Terauds and Lee, 2016) but is made up almost entirely of the ice-covered land mass, coastal tundra and sea ice surrounding the main continent. It contains two additional marine bioregions – the Antarctic Peninsula and Scotia Sea and the Subantarctic Indian Ocean Islands (Chown and Convey, 2007). A bioregion is smaller in scale than a biogeographical realm but larger than an eco-region or an ecosystem, it allows the integrations of multiple eco-regions, including terrestrial, freshwater and marine, into a cohesive system. Whilst these definitions may be challenging in the context of atmospheric biogeochemistry, we argue that a better comprehension of the interactions between the biosphere and the geosphere is needed to better understand aerosol sources in Antarctica.

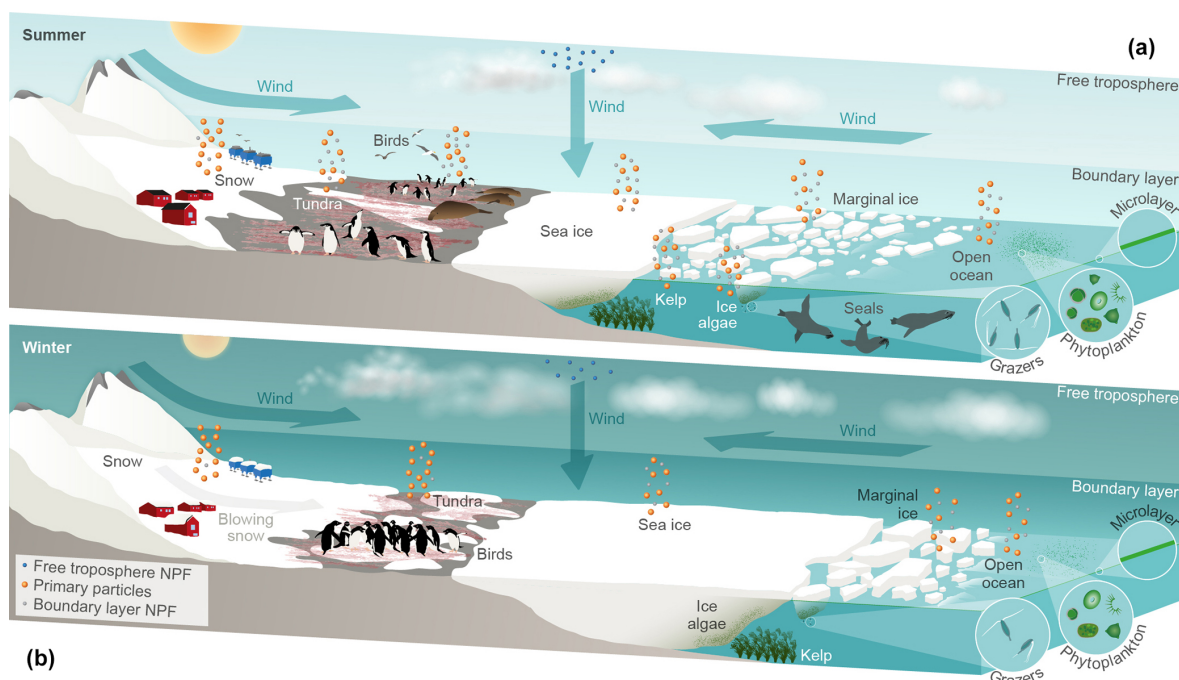


Figure 7. Schematic illustrations of the sea ice, microbiota, sea-to-air emissions, and primary and secondary aerosols in Antarctica during summer (a) and winter (b).

The changes occurring in the Antarctic environment will modify the climate with feedbacks and exchanges between the biosphere and cryosphere with the atmosphere. Changes in marine and terrestrial life – including adaptation of eco-physiology, food and nutrient availability – will affect the emissions of primary and secondary aerosol precursors. Interdisciplinary studies and international cooperation in Antarctica are reducing the gap in our knowledge of these key environmental factors.

Code and data availability. The code and data used to produce all non-illustrative figures are available from the corresponding authors under reasonable request.

Supplement. The supplement related to this article is available online at: <https://doi.org/10.5194/acp-25-1145-2025-supplement>.

Author contributions. Conceptualisation: MD’O conceptualised the paper following the study of Lachlan-Cope et al. (2020). Data curation: EA provided data for Marambio; TLC and AJ provided data for Halley; AL, AV and PA provided data for Dome C; and JP and YJY provided data for King Sejong. Software: DCSB and JB. Formal analysis: DCSB, JB, MD’O. Methodology: DCSB, JB. Project administration: MD’O. Validation: validated by all co-authors. Visualisation: JB. Writing: JB, MD’O. Review and editing: all authors.

Competing interests. At least one of the (co-)authors is a member of the editorial board of *Atmospheric Chemistry and Physics*. The peer-review process was guided by an independent editor, and the authors also have no other competing interests to declare.

Disclaimer. Publisher’s note: Copernicus Publications remains neutral with regard to jurisdictional claims made in the text, published maps, institutional affiliations, or any other geographical representation in this paper. While Copernicus Publications makes every effort to include appropriate place names, the final responsibility lies with the authors.

Acknowledgements. This work acknowledges the “Severo Ochoa Centre of Excellence” accreditation (CEX2019-000928-S). The National Centre for Atmospheric Science (NCAS) Birmingham group is funded by the UK Natural Environment Research Council. The Antarctic cruise PEGASO was led by Rafel Simó (ICM-CSIC). We also thank Chantal Jackson at the GEES Drawing Office from the University of Birmingham (UK).

Financial support. The study was supported by the Spanish Ministry of Economy through the Agencia Estatal de Investigación projects PI-ICE (CTM2017–89117-R) and POLAR-CHANGE (PID2019-110288RB-I00) and the National Centre for Atmospheric Science funded by the Natural Environment Research Council. The publication fee was supported by the CSIC Open Access Publication Support Initiative through its Unit of Information Resources for Research (URICI). Additional sources come from

the Research Council of Finland (decision nos. 335844, 346372). Eija Asmi, Ari Virkkula and Mikko Sipilä were supported by the Academy of Finland project Antarctic Climate Forcing Aerosol (ACFA) (decision no. 335845).

The article processing charges for this open-access publication were covered by the CSIC Open Access Publication Support Initiative through its Unit of Information Resources for Research (URICI).

Review statement. This paper was edited by Manish Shrivastava and reviewed by two anonymous referees.

References

- Amsler C. D., Amsler, K., Iken, J. B., McClintock, M. O., Amsler, K. J., Peters, J. M., Hubbard, F. B., and Furrow, B. J.: Baker Comprehensive evaluation of the palatability and chemical defenses of subtidal macroalgae from the Antarctic Peninsula, *Mar. Ecol. Prog. Ser.*, 294, 141–159, 2005.
- Arrigo, K. R., Lizotte, M. P., and Mock, T.: Primary producers and sea ice, *Science*, 276, 394–397, <https://doi.org/10.1126/science.276.5311.394>, 2009.
- Arrigo, K. R., van Dijken, G. L., and Strong, A. L.: Environmental controls of marine productivity hot spots around Antarctica, *J. Geophys. Res.-Oceans*, 120, 5545–5565, 2015.
- Asmi, E., Frey, A., Virkkula, A., Ehn, M., Manninen, H. E., Timonen, H., Tolonen-Kivimäki, O., Aurela, M., Hillamo, R., and Kulmala, M.: Hygroscopicity and chemical composition of Antarctic sub-micrometre aerosol particles and observations of new particle formation, *Atmos. Chem. Phys.*, 10, 4253–4271, <https://doi.org/10.5194/acp-10-4253-2010>, 2010.
- Atkinson, H. M., Huang, R.-J., Chance, R., Roscoe, H. K., Hughes, C., Davison, B., Schönhardt, A., Mahajan, A. S., Saiz-Lopez, A., Hoffmann, T., and Liss, P. S.: Iodine emissions from the sea ice of the Weddell Sea, *Atmos. Chem. Phys.*, 12, 11229–11244, <https://doi.org/10.5194/acp-12-11229-2012>, 2012.
- Baccarini, A., Karlsson, L., Dommen, J., Duplessis, P., Vüllers, J., Brooks, I. M., Saiz-lopez, A., Salter, M., Tjernström, M., Baltensperger, U., Zieger, P., and Schmale, J.: Frequent new particle formation over the high Arctic pack ice by enhanced iodine emissions, *Nat. Commun.*, 11, 4924, <https://doi.org/10.1038/s41467-020-18551-0>, 2020.
- Baccarini, A., Dommen, J., Lehtipalo, K., Henning, S., Modini, R. L., Geysel-Beer, M., Baltensperger, U., and Schmale, J.: Low-Volatility Vapors and New Particle Formation Over the Southern Ocean During the Antarctic Circumnavigation Expedition, *J. Geophys. Res.-Atmos.*, 126, e2021JD035126, <https://doi.org/10.1029/2021JD035126>, 2021.
- Beddows, D. C. S., Dall'Osto, M., Harrison, R. M., Dall'Osto, M., Harrison, R. M., Dall'Osto, M., and Harrison, R. M.: Cluster Analysis of Rural, Urban, and Curbside Atmospheric Particle Size Data, *Environ. Sci. Technol.*, 43, 4694–4700, <https://doi.org/10.1021/es803121t>, 2009.
- Brean, J., Dall'Osto, M., Simó, R., Shi, Z., Beddows, D. C. S., and Harrison, R. M.: Open ocean and coastal new particle formation from sulfuric acid and amines around the Antarctic Peninsula, *Nat. Geosci.*, 14, 383–388, <https://doi.org/10.1038/s41561-021-00751-y>, 2021.
- Brean, J., Beddows, D. C. S., Harrison, R. M., Song, C., Tunved, P., Ström, J., Krejci, R., Freud, E., Massling, A., Skov, H., Asmi, E., Lupi, A., and Dall'Osto, M.: Collective geographical ecoregions and precursor sources driving Arctic new particle formation, *Atmos. Chem. Phys.*, 23, 2183–2198, <https://doi.org/10.5194/acp-23-2183-2023>, 2023.
- Carslaw, K. S., Lee, L. A., Reddington, C. L., Pringle, K. J., Rap, A., Forster, P. M., Mann, G. W., Spracklen, D. V., Woodhouse, M. T., Regayre, L. A., and Pierce, J. R.: Large contribution of natural aerosols to uncertainty in indirect forcing, *Nature*, 503, 67–71, <https://doi.org/10.1038/nature12674>, 2013.
- Clem, K. R., Fogt, R. L., Turner, J., Lintner, B. R., Marshall, G. J., Miller, J. R., and Renwick, J. A.: Record warming at the South Pole during the past three decades, *Nat. Clim. Change*, 10, 762–770, <https://doi.org/10.1038/s41558-020-0815-z>, 2020.
- Chen, J. L., Wilson, C. R., Blankenship, D., and Tapley, B. D.: Accelerated Antarctic ice loss from satellite gravity measurements, *Nat. Geosci.*, 2, 859–862, <https://doi.org/10.1038/ngeo694>, 2009.
- Chen, X., Virkkula, A., Kerminen, V.-M., Manninen, H. E., Busetto, M., Lanconelli, C., Lupi, A., Vitale, V., Del Guasta, M., Gri-gioni, P., Väänänen, R., Duplissy, E.-M., Petäjä, T., and Kulmala, M.: Features in air ions measured by an air ion spectrometer (AIS) at Dome C, *Atmos. Chem. Phys.*, 17, 13783–13800, <https://doi.org/10.5194/acp-17-13783-2017>, 2017.
- Chown, S. L. and Convey, P.: Spatial and temporal variability across life's hierarchies in the terrestrial Antarctic, *Philos. T. Roy. Soc. B*, 362, 2307–2331, 2007.
- Cunliffe, M., Engel, A., Frka, S., Gasparovic, B., Guitart, C., Murrell, J. C., Salter, M., and Stolle, C.: Sea surface microlayers: A unified physicochemical and biological perspective of the air-ocean interface, *Prog. Oceanogr.*, 1109, 104–116, 2013.
- Dall'Osto, M., Ovadnevaite, J., Paglione, M., Beddows, D. C. S., Ceburnis, D., Cree, C., Cortés, P., Zamanillo, M., Nunes, S. O., Pérez, G. L., Ortega-Retuerta, E., Emelianov, M., Vaqué, D., Marrasé, C., Estrada, M., Sala, M. M., Vidal, M., Fitzsimons, M. F., Beale, R., Ains, R., Rinaldi, M., Decesari, S., Facchini, M. C., Harrison, R. M., O'Dowd, C., and Simó, R.: Antarctic sea ice region as a source of biogenic organic nitrogen in aerosols, *Sci. Rep.*, 7, 6047, <https://doi.org/10.1038/s41598-017-06188-x>, 2017a.
- Dall'Osto, M., Beddows, D. C. S., Tunved, P., Krejci, R., Ström, J., Hansson, H. C., Yoon, Y. J., Park, K. T., Becagli, S., Udusti, R., Onasch, T., O'Dowd, C. D., Simó, R., and Harrison, R. M.: Arctic sea ice melt leads to atmospheric new particle formation, *Sci. Rep.*, 7, 3318, <https://doi.org/10.1038/s41598-017-03328-1>, 2017b.
- Dall'Osto, M., Geels, C., Beddows, D. C. S., Boertmann, D., Lange, R., Nøjgaard, J. K., Harrison, R. M., Simo, R., Skov, H., and Massling, A.: Regions of open water and melting sea ice drive new particle formation in North East Greenland OPEN, *Sci. Rep.*, 8, 6109, <https://doi.org/10.1038/s41598-018-24426-8>, 2018.
- Dall'Osto, M., Ains, R. L., Beale, R., Cree, C., Fitzsimons, M. F., Beddows, D., Harrison, R. M., Ceburnis, D., O'Dowd, C., Rinaldi, M., Paglione, M., Nenes, A., Decesari, S., and Simó, R.: Simultaneous Detection of Alkylamines in

- the Surface Ocean and Atmosphere of the Antarctic Sym-
pagic Environment, *ACS Earth Space Chem.*, 3, 854–862,
<https://doi.org/10.1021/acsearthspacechem.9b00028>, 2019a.
- Dall'Osto, M., Beddows, D. C. S., Tunved, P., Harrison, R. M.,
Lupi, A., Vitale, V., Becagli, S., Traversi, R., Park, K.-T., Yoon,
Y. J., Massling, A., Skov, H., Lange, R., Strom, J., and Krejci,
R.: Simultaneous measurements of aerosol size distributions at
three sites in the European high Arctic, *Atmos. Chem. Phys.*, 19,
7377–7395, <https://doi.org/10.5194/acp-19-7377-2019>, 2019b.
- Dall'Osto, M., Vaqu e, D., Sotomayor-Garcia, A., Cabrera-Brufau,
M., Estrada, M., Buchaca, T., Soler, M., Nunes, S., Zeppen-
feld, S., van Pinxteren, M., Herrmann, H., Wex, H., Rinaldi, M.,
Paglione, M., Beddows, C. S., Harrison, R. M., and Berdalet,
E.: Sea Ice Microbiota in the Antarctic Peninsula Modulates
Cloud-Relevant Sea Spray Aerosol Production, *Front. Mar. Sci.*,
9, 827061, <https://doi.org/10.3389/fmars.2022.827061>, 2022a.
- Dall'Osto, M., Vaqu e, D., Sotomayor-Garcia, A., Cabrera-Brufau,
M., Estrada, M., Buchaca, T., Soler, M., Nunes, S., Zeppen-
feld, S., van Pinxteren, M., Herrmann, H., Wex, H., Rinaldi, M.,
Paglione, M., Beddows, D. C. S., Harrison, R. M., and Berdalet,
E.: Sea ice microbiota in the Antarctic Peninsula modulates
cloud-relevant sea spray aerosol production, *Front. Mar. Sci.*, 9,
827061, <https://doi.org/10.3389/fmars.2022.827061>, 2022b.
- Decesari, S., Paglione, M., Rinaldi, M., Dall'Osto, M., Sim o, R.,
Zanca, N., Volpi, F., Facchini, M. C., Hoffmann, T., G tz,
S., Kampf, C. J., O'Dowd, C., Ceburnis, D., Ovadnevaite, J.,
and Tagliavini, E.: Shipborne measurements of Antarctic sub-
micron organic aerosols: an NMR perspective linking multiple
sources and bioregions, *Atmos. Chem. Phys.*, 20, 4193–4207,
<https://doi.org/10.5194/acp-20-4193-2020>, 2020.
- De Leeuw, G., Andreas, E. L., Anguelova, M. D., Fairall, C. W.,
Lewis, E. R., O'Dowd, C., Schulz, M., and Schwartz, S. E.: Pro-
duction flux of sea spray aerosol, *Rev. Geophys.*, 49, RG2001,
<https://doi.org/10.1029/2010RG000349>, 2011.
- Draxler, R. R. and Rolph, G. D.: HYSPLIT (HYbrid Single-Particle
Lagrangian Integrated Trajectory) Model, NOAA ARL READY
Website, <https://www.ready.noaa.gov/HYSPLIT.php> (last access:
4 February 2024), 2010.
- Fetterer, F., Knowles, K., Meier, W. N., Savoie, M., and Wind-
nagel, A. K.: Sea Ice Index, Version 3, National Snow and
Ice Data Center (NSIDC) [data set], Boulder, Colorado, USA,
<https://doi.org/10.7265/N5K072F8>, 2017.
- Fiebig, M., Hirdman, D., Lunder, C. R., Ogren, J. A., Sol-
berg, S., Stohl, A., and Thompson, R. L.: Annual cycle
of Antarctic baseline aerosol: controlled by photooxidation-
limited aerosol formation, *Atmos. Chem. Phys.*, 14, 3083–3093,
<https://doi.org/10.5194/acp-14-3083-2014>, 2014.
- Fossum, K. N., Ovadnevaite, J., Ceburnis, D., Dall'Osto, M.,
Marullo, S., Bellacicco, M., Sim o, R., Liu, D., Flynn, M.,
Zuend, A., and O'Dowd, C.: Summertime Primary and Sec-
ondary Contributions to Southern Ocean Cloud Condensation
Nuclei, *Sci. Rep.*, 8, 13844, <https://doi.org/10.1038/s41598-018-32047-4>, 2018.
- Frey, M. M., Norris, S. J., Brooks, I. M., Anderson, P. S., Nishimura,
K., Yang, X., Jones, A. E., Nerentorp Mastromonaco, M. G.,
Jones, D. H., and Wolff, E. W.: First direct observation of sea
salt aerosol production from blowing snow above sea ice, *At-
mos. Chem. Phys.*, 20, 2549–2578, <https://doi.org/10.5194/acp-20-2549-2020>, 2020.
- Gantt, B. and Meskhidze, N.: The physical and chemical char-
acteristics of marine primary organic aerosol: a review, *At-
mos. Chem. Phys.*, 13, 3979–3996, <https://doi.org/10.5194/acp-13-3979-2013>, 2013.
- Giordano, M. R., Kalnajs, L. E., Goetz, J. D., Avery, A. M., Katz,
E., May, N. W., Leemon, A., Mattson, C., Pratt, K. A., and
DeCarlo, P. F.: The importance of blowing snow to halogen-
containing aerosol in coastal Antarctica: influence of source re-
gion versus wind speed, *Atmos. Chem. Phys.*, 18, 16689–16711,
<https://doi.org/10.5194/acp-18-16689-2018>, 2018.
- Gras, J. L. and Keywood, M.: Cloud condensation nuclei over
the Southern Ocean: wind dependence and seasonal cycles, *At-
mos. Chem. Phys.*, 17, 4419–4432, <https://doi.org/10.5194/acp-17-4419-2017>, 2017.
- Gong, X., Zhang, J., Croft, B., Yang, X., Frey, M. M., Bergner, N.,
Chang, R. Y.-W., Creamean, J. M., Kuang, C., Martin, R. V., Ran-
jithkumar, A., Sedlacek, A. J., Uin, J., Willmes, S., Zawadowicz,
M. A., Pierce, J. R., Shupe, M. D., Schmale, J., and Wang, J.:
Arctic warming by abundant fine sea salt aerosols from blowing
snow, *Nat. Geosci.* 16, 768–774, <https://doi.org/10.1038/s41561-023-01254-8>, 2023.
- Hamilton, D. S., Lee, L. A., Pringle, K. J., Reddington,
C. L., Spracklen, D. V., and Carslaw, K. S.: Occur-
rence of pristine aerosol environments on a polluted
planet, *P. Natl. Acad. Sci. USA*, 111, 18466–18471,
<https://doi.org/10.1073/pnas.1415440111>, 2014.
- Hara, K., Osada, K., Nishita-Hara, C., and Yamanouchi, T.: Sea-
sonal variations and vertical features of aerosol particles in the
Antarctic troposphere, *Atmos. Chem. Phys.*, 11, 5471–5484,
<https://doi.org/10.5194/acp-11-5471-2011>, 2011.
- Hara, K., Nishita-Hara, C., Osada, K., Yabuki, M., and Ya-
manouchi, T.: Characterization of aerosol number size dis-
tributions and their effect on cloud properties at Syowa
Station, Antarctica, *Atmos. Chem. Phys.*, 21, 12155–12172,
<https://doi.org/10.5194/acp-21-12155-2021>, 2021.
- He, X.-C., Tham, Y. J., Dada, L., Wang, M., Finkenzeller, H.,
Stolzenburg, D., Iyer, S., Simon, M., K rten, A., Shen, J., R rup,
B., Rissanen, M., Schobesberger, S., Baalbaki, R., Wang, D. S.,
Koenig, T. K., Jokinen, T., Sarnela, N., Beck, L. J., Almeida, J.,
Amanatidis, S., Amorim, A., Ataei, F., Baccarini, A., Bertozzi,
B., Bianchi, F., Brilke, S., Caudillo, L., Chen, D., Chiu, R., Chu,
B., Dias, A., Ding, A., Dommen, J., Duplissy, J., El Haddad, I.,
Gonzalez Carracedo, L., Granzin, M., Hansel, A., Heinritzi, M.,
Hofbauer, V., Junninen, H., Kangasluoma, J., Kempainen, D.,
Kim, C., Kong, W., Krechmer, J. E., Kvashin, A., Laitinen, T.,
Lamkaddam, H., Lee, C. P., Lehtipalo, K., Leiminger, M., Li, Z.,
Makhmutov, V., Manninen, H. E., Marie, G., Marten, R., Mathot,
S., Mauldin, R. L., Mentler, B., M hler, O., M ller, T., Nie,
W., Onnela, A., Pet j , T., Pfeifer, J., Philippov, M., Ranjithku-
mar, A., Saiz-Lopez, A., Salma, I., Scholz, W., Schuchmann,
S., Schulze, B., Steiner, G., Stozhkov, Y., Tauber, C., Tom , A.,
Thakur, R. C., V is nen, O., Vazquez-Pufleau, M., Wagner, A. C.,
Wang, Y., Weber, S. K., Winkler, P. M., Wu, Y., Xiao, M.,
Yan, C., Ye, Q., Ylisirni , A., Zauner-Wieczorek, M., Zha, Q.,
Zhou, P., Flagan, R. C., Curtius, J., Baltensperger, U., Kulmala,
M., Kerminen, V.-M., Kurt n, T., Donahue, N. M., Volkamer,
R., Kirkby, J., Worsnop, D. R., and Sipil , M.: Role of iodine
oxoacids in atmospheric aerosol nucleation, *Science*, 371, 589–
595, <https://doi.org/10.1126/science.abe0298>, 2021.

- He, X.-C., Simon, M., Iyer, S., Xie, H.-B., Rörup, B., Shen, J., Finkenzeller, H., Stolzenburg, D., Zhang, R., Baccarini, A., Tham, Y. J., Wang, M., Amanatidis, S., Piedehierro, A. A., Amorim, A., Baalbaki, R., Brasseur, Z., Caudillo, L., Chu, B., Dada, L., Duplissy, J., El Haddad, I., Flagan, R. C., Granzin, M., Hansel, A., Heinritzi, M., Hofbauer, V., Jokinen, T., Kempainen, D., Kong, W., Krechmer, J., Kürten, A., Lamkaddam, H., Lopez, B., Ma, F., Mahfouz, N. G. A., Makhmutov, V., Manninen, H. E., Marie, G., Marten, R., Massabò, D., Mauldin, R. L., Mentler, B., Onnela, A., Petäjä, T., Pfeifer, J., Philippov, M., Ranjithkumar, A., Rissanen, M. P., Schobesberger, S., Scholz, W., Schulze, B., Surdu, M., Thakur, R. C., Tomé, A., Wagner, A. C., Wang, D., Wang, Y., Weber, S. K., Welti, A., Winkler, P. M., Zauner-Wieczorek, M., Baltensperger, U., Curtius, J., Kurtén, T., Worsnop, D. R., Volkamer, R., Lehtipalo, K., Kirkby, J., Donahue, N. M., Sipilä, M., and Kulmala, M.: Iodine oxoacids enhance nucleation of sulfuric acid particles in the atmosphere, *Science*, 382, 1308–1314, <https://doi.org/10.1126/science.adh2526>, 2023.
- Heinrichs, M. E., Piedade, G. J., Popa, O., Sommers, P., Trubl, G., Weissenbach, J., and Rahlf, J.: Breaking the Ice: A Review of Phages in Polar Ecosystems, in: *Bacteriophages. Methods in Molecular Biology*, edited by: Tumban, E., Humana, New York, NY, 2738, 31–71, https://doi.org/10.1007/978-1-0716-3549-0_3, 2024.
- Heintzenberg, J., Covert, D. S., and Van Dingenen, R.: Size distribution and chemical composition of marine aerosols: A compilation and review, *Tellus B*, 52, 1104–1122, <https://doi.org/10.3402/tellusb.v52i4.17090>, 2000.
- Heintzenberg, J., Legrand, M., Gao, Y., Hara, K., Huang, S., Humphries, R. S., Kamra, A. K., Keywood, M. D., and Sakerin, S. M.: Spatio-Temporal Distributions of the Natural Non-Sea-Salt Aerosol Over the Southern Ocean and Coastal Antarctica and Its Potential Source Regions, *Tellus B*, 75, 47–64, <https://doi.org/10.16993/tellusb.1869>, 2023.
- Herenz, P., Wex, H., Mangold, A., Laffineur, Q., Gorodetskaya, I. V., Fleming, Z. L., Panagi, M., and Stratmann, F.: CCN measurements at the Princess Elisabeth Antarctica research station during three austral summers, *Atmos. Chem. Phys.*, 19, 275–294, <https://doi.org/10.5194/acp-19-275-2019>, 2019.
- Hoppel, W. A., Frick, G. M., and Fitzgerald, J. W.: Marine boundary layer measurements of new-particle formation and the effects of non-precipitating clouds have on aerosol size distribution, *J. Geophys. Res.*, 99, 14443–14459, 1994.
- Hsu, Y., Holsen, T. M., and Hopke, P. K.: Comparison of hybrid receptor models to locate PCB sources in Chicago, *Atmos. Environ.*, 37, 545–562, 2003.
- Humphries, R. S., Schofield, R., Keywood, M. D., Ward, J., Pierce, J. R., Gionfriddo, C. M., Tate, M. T., Krabbenhoft, D. P., Galbally, I. E., Molloy, S. B., Klekociuk, A. R., Johnston, P. V., Kreher, K., Thomas, A. J., Robinson, A. D., Harris, N. R. P., Johnson, R., and Wilson, S. R.: Boundary layer new particle formation over East Antarctic sea ice – possible Hg-driven nucleation?, *Atmos. Chem. Phys.*, 15, 13339–13364, <https://doi.org/10.5194/acp-15-13339-2015>, 2015.
- Humphries, R. S., Keywood, M. D., Gribben, S., McRobert, I. M., Ward, J. P., Selleck, P., Taylor, S., Harnwell, J., Flynn, C., Kulkarni, G. R., Mace, G. G., Protat, A., Alexander, S. P., and McFarquhar, G.: Southern Ocean latitudinal gradients of cloud condensation nuclei, *Atmos. Chem. Phys.*, 21, 12757–12782, <https://doi.org/10.5194/acp-21-12757-2021>, 2021.
- Humphries, R. S., Keywood, M. D., Ward, J. P., Harnwell, J., Alexander, S. P., Klekociuk, A. R., Hara, K., McRobert, I. M., Protat, A., Alroe, J., Cravigan, L. T., Miljevic, B., Ristovski, Z. D., Schofield, R., Wilson, S. R., Flynn, C. J., Kulkarni, G. R., Mace, G. G., McFarquhar, G. M., Chambers, S. D., Williams, A. G., and Griffiths, A. D.: Measurement report: Understanding the seasonal cycle of Southern Ocean aerosols, *Atmos. Chem. Phys.*, 23, 3749–3777, <https://doi.org/10.5194/acp-23-3749-2023>, 2023.
- Ito, T.: Size distribution of Antarctic submicron aerosols, *Tellus B*, 45, 145–59, 1993.
- James, I. M.: The Antarctic drainage flow: implications for hemispheric flow on the Southern Hemisphere, *Antarct. Sci.*, 1, 279–290, 1989.
- Jang, E., Park, K.-T., Yoon, Y. J., Kim, T.-W., Hong, S.-B., Becagli, S., Traversi, R., Kim, J., and Gim, Y.: New particle formation events observed at the King Sejong Station, Antarctic Peninsula – Part 2: Link with the oceanic biological activities, *Atmos. Chem. Phys.*, 19, 7595–7608, <https://doi.org/10.5194/acp-19-7595-2019>, 2019.
- Järvinen, E., Virkkula, A., Nieminen, T., Aalto, P. P., Asmi, E., Landonelli, C., Busetto, M., Lupi, A., Schioppa, R., Vitale, V., Mazzola, M., Petäjä, T., Kerminen, V.-M., and Kulmala, M.: Seasonal cycle and modal structure of particle number size distribution at Dome C, Antarctica, *Atmos. Chem. Phys.*, 13, 7473–7487, <https://doi.org/10.5194/acp-13-7473-2013>, 2013.
- Jokinen, T., Sipilä, M., Kontkanen, J., Vakkari, V., Tisler, P., Duplissy, E.-M., Junninen, H., Kangasluoma, J., Manninen, H. E., Petäjä, T., Kulmala, M., Worsnop, D. R., Kirkby, J., Virkkula, A., and Kerminen, V.-M.: Ion-induced sulfuric acid–ammonia nucleation drives particle formation in coastal Antarctica, *Science Advances*, 4, eaat9744, <https://doi.org/10.1126/sciadv.aat9744>, 2018.
- Kerminen, V. M., Chen, X., Vakkari, V., Petäjä, T., Kulmala, M., and Bianchi, F.: Atmospheric new particle formation and growth: Review of field observations, *Environ. Res. Lett.*, 13, 103003, <https://doi.org/10.1088/1748-9326/aadf3c>, 2018.
- Kim, J., Yoon, Y. J., Gim, Y., Kang, H. J., Choi, J. H., Park, K.-T., and Lee, B. Y.: Seasonal variations in physical characteristics of aerosol particles at the King Sejong Station, Antarctic Peninsula, *Atmos. Chem. Phys.*, 17, 12985–12999, <https://doi.org/10.5194/acp-17-12985-2017>, 2017.
- Kim, J., Yoon, Y. J., Gim, Y., Choi, J. H., Kang, H. J., Park, K.-T., Park, J., and Lee, B. Y.: New particle formation events observed at King Sejong Station, Antarctic Peninsula – Part 1: Physical characteristics and contribution to cloud condensation nuclei, *Atmos. Chem. Phys.*, 19, 7583–7594, <https://doi.org/10.5194/acp-19-7583-2019>, 2019.
- Kirkby, J., Curtius, J., Almeida, J., Dunne, E., Duplissy, J., Ehrhart, S., Franchin, A., Gagné, S., Ickes, L., Kürten, A., Kupc, A., Metzger, A., Riccobono, F., Rondo, L., Schobesberger, S., Tsagko-georgas, G., Wimmer, D., Amorim, A., Bianchi, F., Breitenlechner, M., David, A., Dommen, J., Downard, A., Ehn, M., Flagan, R. C., Haider, S., Hansel, A., Hauser, D., Jud, W., Junninen, H., Kreissl, F., Kvashin, A., Laaksonen, A., Lehtipalo, K., Lima, J., Lovejoy, E. R., Makhmutov, V., Mathot, S., Mikkilä, J., Minginette, P., Mogo, S., Nieminen, T., Onnela, A., Pereira, P.,

- Petäjä, T., Schnitzhofer, R., Seinfeld, J. H., Sipilä, M., Stozhkov, Y., Stratmann, F., Tomé, A., Vanhanen, J., Viisanen, Y., Virtala, A., Wagner, P. E., Walther, H., Weingartner, E., Wex, H., Winkler, P. M., Carslaw, K. S., Worsnop, D. R., Baltensperger, U., and Kulmala, M.: Role of sulphuric acid, ammonia and galactic cosmic rays in atmospheric aerosol nucleation, *Nature*, 476, 429–435, <https://doi.org/10.1038/nature10343>, 2011.
- Koponen, I. K., Virkkula, A., Hillamo, R., Kerminen, V.-M., and Kulmala, M.: Number size distributions of marine aerosols: observations during a cruise between the English Channel and coast of Antarctica, *J. Geophys. Res.*, 107, 4753, <https://doi.org/10.1029/2002JD002533>, 2002.
- Korhonen, H., Carslaw, K. S., Spracklen, D. V., Mann, G. W., and Woodhouse, M. T.: Influence of oceanic dimethyl sulfide emissions on cloud condensation nuclei concentrations and seasonality over the remote Southern Hemisphere oceans: A global model study, *J. Geophys. Res.-Atmos.*, 113, D15204, <https://doi.org/10.1029/2007JD009718>, 2008.
- Lachlan-Cope, T., Beddows, D. C. S., Brough, N., Jones, A. E., Harrison, R. M., Lupi, A., Yoon, Y. J., Virkkula, A., and Dall'Osto, M.: On the annual variability of Antarctic aerosol size distributions at Halley Research Station, *Atmos. Chem. Phys.*, 20, 4461–4476, <https://doi.org/10.5194/acp-20-4461-2020>, 2020.
- Lana, A., Bell, T. G., Simo, R., Vallina, S. M., Ballabrera-Poy, J., Kettle, A. J., Dachs, J., Bopp, L., Saltzman, E. S., Stefels, J., Johnson, J. E., and Liss, P. S.: An updated climatology of surface dimethylsulfide concentrations and emission fluxes in the global ocean, *Global Biogeochem. Cy.*, 25, GB1004, <https://doi.org/10.1029/2010GB003850>, 2011.
- Lapere, R., Thomas, J. L., Marelle, L., Ekman, A. M. L., Frey, M. M., Lund, M. T., Makkonen, R., Ranjithkumar, A., Salter, M. E., Samset, B. H., Schulz, M., Sogacheva, L., Yang, X., and Zieger, P.: The representation of sea salt aerosols and their role in polar climate within CMIP6, *J. Geophys. Res.-Atmos.*, 128, e2022JD038235, <https://doi.org/10.1029/2022JD038235>, 2023.
- Lee, S. H., Gordon, H., Yu, H., Lehtipalo, K., Haley, R., Li, Y., and Zhang, R.: New Particle Formation in the Atmosphere: From Molecular Clusters to Global Climate, *J. Geophys. Res.-Atmos.*, 124, 7098–7146, <https://doi.org/10.1029/2018JD029356>, 2019.
- Legrand, M., Yang, X., Preunkert, S., and Theys, N.: Year-round records of sea salt, gaseous, and particulate inorganic bromine in the atmospheric boundary layer at coastal (Dumont d'Urville) and central (Concordia) East Antarctic sites, *J. Geophys. Res.-Atmos.*, 121, 997–1023, 2016.
- Lupu, A. and Maenhaut, W.: Application and comparison of two statistical trajectory techniques for identification of source regions of atmospheric aerosol species, *Atmos. Environ.*, 36, 5607–5618, 2002.
- McCoy, D. T., Burrows, S. M., Wood, R., Grosvenor, D. P., Elliott, S. M., Ma, P. L., Rasch, P. J., and Hartmann, D. L.: Natural aerosols explain seasonal and spatial patterns of Southern Ocean cloud albedo, *Science Advances*, 1, e1500157, <https://doi.org/10.1126/sciadv.1500157>, 2015.
- Meskhize, N. and Nenes, A.: Phytoplankton and cloudiness in the Southern Ocean, *Science*, 314, 1419–1423, <https://doi.org/10.1126/science.1131779>, 2006.
- Mungall, E. L., Abbatt, J. P. D., Wentzell, J. J. B., Lee, A. K. Y., Thomas, J. L., Blais, M., Gosselin, M., Miller, L. A., Papakyriakou, T., Willis, M. D., and Liggio, J.: Microlayer source of oxygenated volatile organic compounds in the summertime marine Arctic boundary layer, *P. Natl. Acad. Sci. USA*, 114, 6203–6208, <https://doi.org/10.1073/pnas.1620571114>, 2017.
- O'Dowd, C. D., Lowe, J. A., Smith, M. H., Davison, B., Hewitt, C. N., and Harrison, R. M.: Biogenic sulphur emissions and inferred non-sea-salt-sulphate particularly during Events of new particle formation in and around Antarctica, *J. Geophys. Res.*, 102, 12839–12854, <https://doi.org/10.1029/96JD02749>, 1997a.
- O'Dowd, C. D., Smith, M. H., Consterdine, I. E., and Lowe, J. A.: Marine aerosol, sea-salt, and the marine sulphur cycle: A short review, *Atmos. Environ.*, 31, 73–80, [https://doi.org/10.1016/S1352-2310\(96\)00106-9](https://doi.org/10.1016/S1352-2310(96)00106-9), 1997b.
- Otero, X. L., De La Peña-Lastra, S., Pérez-Alberti, A., Ferreira, T. O., and Huerta-Díaz, M. A.: Seabird colonies as important global drivers in the nitrogen and phosphorus cycles, *Nat. Commun.*, 9, 246, <https://doi.org/10.1038/s41467-017-02446-8>, 2018.
- Paglione, M., Beddows, D. C. S., Jones, A., Lachlan-Cope, T., Rinaldi, M., Decesari, S., Manarini, F., Russo, M., Mansour, K., Harrison, R. M., Mazzanti, A., Tagliavini, E., and Dall'Osto, M.: Simultaneous organic aerosol source apportionment at two Antarctic sites reveals large-scale and ecoregion-specific components, *Atmos. Chem. Phys.*, 24, 6305–6322, <https://doi.org/10.5194/acp-24-6305-2024>, 2024.
- Park, J., Kang, H., Gim, Y., Jang, E., Park, K.-T., Park, S., Jung, C. H., Ceburnis, D., O'Dowd, C., and Yoon, Y. J.: New particle formation leads to enhanced cloud condensation nuclei concentrations on the Antarctic Peninsula, *Atmos. Chem. Phys.*, 23, 13625–13646, <https://doi.org/10.5194/acp-23-13625-2023>, 2023.
- Peck, L. S.: Antarctic marine biodiversity: adaptations, environments and responses to change, *Oceanogr. Mar. Biol.*, 56, 105–236, 2018.
- Quéléver, L. L. J., Dada, L., Asmi, E., Lampilahti, J., Chan, T., Ferrara, J. E., Copes, G. E., Pérez-Fogwill, G., Barreira, L., Aurela, M., Worsnop, D. R., Jokinen, T., and Sipilä, M.: Investigation of new particle formation mechanisms and aerosol processes at Marambio Station, Antarctic Peninsula, *Atmos. Chem. Phys.*, 22, 8417–8437, <https://doi.org/10.5194/acp-22-8417-2022>, 2022.
- Quinn, P. K. and Bates, T. S.: The case against climate regulation via oceanic phytoplankton sulphur emissions, *Nature*, 480, 51–56, <https://doi.org/10.1038/nature10580>, 2011.
- Rankin, A. M. and Wolff, E. W.: A year-long record of size-segregated aerosol composition at Halley, Antarctica, *J. Geophys. Res.-Atmos.*, 108, 4775, <https://doi.org/10.1029/2003JD003993>, 2003.
- Reddington, C. L., Carslaw, K. S., Stier, P., Schutgens, N., Coe, H., Liu, D., Allan, J., Browse, J., Pringle, K. J., Lee, L. A., Yoshioka, M., Johnson, J. S., Regayre, L. A., Spracklen, D. V., Mann, G. W., Clarke, A., Hermann, M., Henning, S., Wex, H., Kristensen, T. B., Leaitch, W. R., Pöschl, U., Rose, D., Andreae, M. O., Schmale, J., Kondo, Y., Oshima, N., Schwarz, J. P., Nenes, A., Anderson, B., Roberts, G. C., Snider, J. R., Leck, C., Quinn, P. K., Chi, X., Ding, A., Jimenez, J. L., and Zhang, Q.: The global aerosol synthesis and science project (GASSP): Measurements and modeling to reduce uncertainty, *B. Am. Meteorol. Soc.*, 98, 1857–1877, <https://doi.org/10.1175/BAMS-D-15-00317.1>, 2017.
- Riddick, S. N., Dragosits, U., Blackall, T. D., Daunt, F., Wanless, S., and Sutton, M. A.: The global distribution of ammonia

- emissions from seabird colonies, *Atmos. Environ.*, 55, 319–327, <https://doi.org/10.1016/j.atmosenv.2012.02.052>, 2012.
- Rinaldi, M., Paglione, M., Decesari, S., Harrison, R. M., Beddows, D. C., Ovadnevaite, J., Ceburnis, D., O'Dowd, C. D., Simó, R., and Dall'Osto, M.: Contribution of Water-Soluble Organic Matter from Multiple Marine Geographic Eco-Regions to Aerosols around Antarctica, *Environ. Sci. Technol.*, 54, 7807–7817, <https://doi.org/10.1021/acs.est.0c00695>, 2020.
- Ronowicz, M., Peña Cantero, A. L., Mercado Casares, B., Kukulinski, P., and Soto Àngel, J. J.: Assessing patterns of diversity, bathymetry and distribution at the poles using hydrozoa (Cnidaria) as a model group, *Hydrobiologia*, 833, 25–51, <https://doi.org/10.1007/s10750-018-3876-5>, 2019.
- Saiz-Lopez, A., Chance, K., Liu, X., Kurosu, T. P., and Sander, S. P.: First observations of iodine oxide from space, *Geophys. Res. Lett.*, 34, L12812, <https://doi.org/10.1029/2007GL030111>, 2007.
- Saliba, G., Sanchez, K. J., Russell, L. M., Twohy, C. H., Roberts, G. C., Lewis, S., Dedrick, J., McCluskey, C. S., Moore, K., DeMott, P. J., and Toohey, D. W.: Organic composition of three different size ranges of aerosol particles over the Southern Ocean, *Aerosol Sci. Tech.*, 55, 268–288, <https://doi.org/10.1080/02786826.2020.1845296>, 2021.
- Schmale, J., Schneider, J., Nemitz, E., Tang, Y. S., Dragosits, U., Blackall, T. D., Trathan, P. N., Phillips, G. J., Sutton, M., and Braban, C. F.: Sub-Antarctic marine aerosol: dominant contributions from biogenic sources, *Atmos. Chem. Phys.*, 13, 8669–8694, <https://doi.org/10.5194/acp-13-8669-2013>, 2013.
- Shaw, G. E.: Considerations on the Origin and Properties of the Antarctic Aerosol, *Rev. Geophys.*, 17, 1983–1998, 1988.
- Sipilä, M., Sarnela, N., Jokinen, T., Henschel, H., Junninen, H., Kontkanen, J., Richters, S., Kangasluoma, J., Franchin, A., Peräkylä, O., Rissanen, M. P., Ehn, M., Vehkamäki, H., Kurten, T., Berndt, T., Petäjä, T., Worsnop, D., Ceburnis, D., Kerminen, V. M., Kulmala, M., and O'Dowd, C.: Molecular-scale evidence of aerosol particle formation via sequential addition of HIO₃, *Nature*, 537, 532–534, <https://doi.org/10.1038/nature19314>, 2016.
- Terauds, A. and Lee, J. R.: Antarctic biogeography revisited: updating the Antarctic conservation biogeographic regions, *Divers. Distrib.*, 22, 836–840, 2016.
- Terauds, A., Chown, S. L., Morgan, F., Peat, H. J., Watts, D. J., Keys, H., Convey, P., and Bergstrom, D. M.: Conservation biogeography of the Antarctic, *Divers. Distrib.*, 18, 726–741, 2012.
- Turner, J., Colwell, S. R., Marshall, G. J., Lachlan-Cope, T. A., Carleton, A. M., Jones, P. D., Lagun, V., Reid, P. A., and Iagovkina, S.: Antarctic climate change during the last 50 years, *Int. J. Climatol.*, 25, 279–294, <https://doi.org/10.1002/joc.1130>, 2005.
- U.S. National Ice Center: IMS Daily Northern Hemisphere Snow and Ice Analysis at 1 km, 4 km, and 24 km Resolutions, Version 1, National Snow and Ice Data Center (NSIDC) [data set], Boulder, Colorado, USA, <https://doi.org/10.7265/N52R3PMC>, 2008.
- Vaqué, D., Boras, J. A., Arrieta, J. M., Agustí, S., Duarte, C. M., and Sala, M. M.: Enhanced Viral Activity in the Surface Microlayer of the Arctic and Antarctic Oceans, *Microorganisms*, 9, 317, <https://doi.org/10.3390/microorganisms9020317>, 2021.
- Virkkula, A., Grythe, H., Backman, J., Petäjä, T., Busetto, M., Lanconelli, C., Lupi, A., Becagli, S., Traversi, R., Severi, M., Vitale, V., Sheridan, P., and Andrews, E.: Aerosol optical properties calculated from size distributions, filter samples and absorption photometer data at Dome C, Antarctica, and their relationships with seasonal cycles of sources, *Atmos. Chem. Phys.*, 22, 5033–5069, <https://doi.org/10.5194/acp-22-5033-2022>, 2022.
- Yang, X., Frey, M. M., Rhodes, R. H., Norris, S. J., Brooks, I. M., Anderson, P. S., Nishimura, K., Jones, A. E., and Wolff, E. W.: Sea salt aerosol production via sublimating wind-blown saline snow particles over sea ice: parameterizations and relevant microphysical mechanisms, *Atmos. Chem. Phys.*, 19, 8407–8424, <https://doi.org/10.5194/acp-19-8407-2019>, 2019.
- Wang, M., Xiao, M., Bertozzi, B., Marie, G., Rörup, B., Schulze, B., Bardakov, R., He, X.-C., Shen, J., Scholz, W., Marten, R., Dada, L., Baalbaki, R., Lopez, B., Lamkaddam, H., Manninen, H. E., Amorim, A., Ataei, F., Bogert, P., Basseur, Z., Caudillo, L., De Menezes, L.-P., Duplissy, J., Ekman, A. M. L., Finkenzeller, H., Carracedo, L. G., Granzin, M., Guida, R., Heinritzi, M., Hofbauer, V., Höhler, K., Korhonen, K., Krechmer, J. E., Kürten, A., Lehtipalo, K., Mahfouz, N. G. A., Makhmutov, V., Massabò, D., Mathot, S., Mauldin, R. L., Mentler, B., Müller, T., Onnela, A., Petäjä, T., Philippov, M., Piedadhierro, A. A., Pozzer, A., Ranjithkumar, A., Schervish, M., Schobesberger, S., Simon, M., Stozhkov, Y., Tomé, A., Umo, N. S., Vogel, F., Wagner, R., Wang, D. S., Weber, S. K., Welti, A., Wu, Y., Zauner-Wieczorek, M., Sipilä, M., Winkler, P. M., Hansel, A., Baltensperger, U., Kulmala, M., Flagan, R. C., Curtius, J., Riipinen, I., Gordon, H., Lelieveld, J., El-Haddad, I., Volkamer, R., Worsnop, D. R., Christoudias, T., Kirkby, J., Möhler, O., and Donahue, N. M.: Synergistic HNO₃–H₂SO₄–NH₃ upper tropospheric particle formation, *Nature*, 605, 483–489, <https://doi.org/10.1038/s41586-022-04605-4>, 2022.
- Weller, R., Minikin, A., Wagenbach, D., and Dreiling, V.: Characterization of the inter-annual, seasonal, and diurnal variations of condensation particle concentrations at Neumayer, Antarctica, *Atmos. Chem. Phys.*, 11, 13243–13257, <https://doi.org/10.5194/acp-11-13243-2011>, 2011.
- Weller, R., Schmidt, K., Teinilä, K., and Hillamo, R.: Natural new particle formation at the coastal Antarctic site Neumayer, *Atmos. Chem. Phys.*, 15, 11399–11410, <https://doi.org/10.5194/acp-15-11399-2015>, 2015.
- Weller, R., Legrand, M., and Preunkert, S.: Size distribution and ionic composition of marine summer aerosol at the continental Antarctic site Kohnen, *Atmos. Chem. Phys.*, 18, 2413–2430, <https://doi.org/10.5194/acp-18-2413-2018>, 2018.
- Wiencke, C. and Amsler, C. D.: Seaweeds and Their Communities in Polar Regions, in: *Seaweed Biology. Ecological Studies*, Springer, Berlin, Heidelberg, 265–291, https://doi.org/10.1007/978-3-642-28451-9_13, 2012.